

50123

NEUTRONICS STUDY OF THE CONVERSION
OF THE UNIVERSITY OF MISSOURI-ROLLA REACTOR
TO LOW ENRICHED URANIUM FUEL

BY

LORNE J. COVINGTON, 1963.

A THESIS

Presented to the Faculty of the Graduate School of the

UNIVERSITY OF MISSOURI-ROLLA

In Partial Fulfillment of the Requirements for the Degree

MASTER OF SCIENCE IN NUCLEAR ENGINEERING

1989

Approved by

M Straka

Dr. Milan Straka, Advisor

D Ray Edwards

Dr. D. Ray Edwards

Albert E. Bolon

Dr. Albert E. Bolon

D C Look, Jr.

Dr. Dwight C. Look, Jr.

01133

A020

011

PUBLICATION THESIS OPTION

This thesis has been prepared in the style utilized by the Journal of Nuclear Technology. Pages 1 - 31 will be presented for publication in that journal. Appendices A - G have been added for the purposes normal to thesis writing.

ACKNOWLEDGEMENTS

My thanks to my advisor Dr. Milan Straka for his guidance, support and encouragement. Special thanks are extended to my committee members Dr. Milan Straka, Dr. D. Ray Edwards, Dr. Albert E. Bolon, and Dr. Dwight C. Look, Jr. for their help in conducting my research.

The author would like to thank Dr. James E. Matos, Dr. Armando Travelli, Dr. William L. Woodruff, and Mr. Roger Rempert of the Reduced Enrichment for Research and Test Reactors Program of the Argonne National Laboratory for their help and guidance. I also want to thank the staff of the University of Missouri-Rolla Reactor Facility for their help.

The author is grateful for the financial support received from the Department of Energy (Grant Number DE-FG02-86ER75272). I am also grateful for the fellowship from the Power Group and also the support from the U.S. Department of Interior.

Many thanks to my wife, Julie, who has given me support and encouragement throughout this research.

Table of Contents

	Page
PUBLICATION THESIS OPTION.....	ii
ACKNOWLEDGEMENTS.....	iii
LIST OF ILLUSTRATIONS.....	vi
LIST OF TABLES.....	viii
NEUTRONICS STUDY OF THE CONVERSION OF THE UNIVERSITY OF MISSOURI-ROLLA REACTOR TO LOW ENRICHED URANIUM FUEL	
ABSTRACT.....	2
I. INTRODUCTION.....	3
II. METHODOLOGY AND CODES.....	5
III. REACTOR CALCULATIONS.....	8
A. Effective Multiplication Factor And Thermal Flux Distribution.....	8
B. Reactivity Coefficients.....	11
C. Irradiation Facilities And Control Rods.....	14
IV. CONCLUSIONS.....	18
ACKNOWLEDGEMENTS.....	19
NOMENCLATURE.....	20
REFERENCES.....	21
ADDITIONAL REFERENCES.....	32
VITA.....	33
APPENDICES.....	34
A. CODE DESCRIPTIONS AND INPUT EXAMPLES.....	34
A1. LEOPARD.....	34
A2. 2DB-UM.....	36
B. CROSS SECTION GENERATION AND CELL DISCRETIZATION.....	41
C. SELECTION OF A LEU CORE CONFIGURATION.....	49

D. CALCULATION OF POWER PEAKING FACTORS AND POWER DISTRIBUTIONS.....	52
E. CALCULATIONS OF REACTIVITY COEFFICIENTS.....	59
F. METHODS TO CALCULATE REACTIVITY WORTHS OF CONTROL RODS.....	66
G. ADDITIONAL REACTIVITY CALCULATIONS.....	70

LIST OF ILLUSTRATIONS

vi

	Page
1. (a) Current HEU and (b) proposed LEU core configurations.....	26
2. Computational models of (a) HEU standard element, (b) LEU control element (not to scale).....	27
3. Calculated and measured lateral thermal neutron flux profiles through row D of the HEU core.....	28
4. Total moderator coefficient for the HEU and LEU cores.....	29
5. Reactivity of the UMRR void tube at the HEU core periphery (C-3).....	30
6. Lateral thermal flux profile along centerline of irradiation fuel element in grid position E-5.....	31
B1. The HEU standard element from UMRP blueprints (shown with top handle).....	44
B2. The HEU control element from UMRR blueprints.....	45
B3. The computational model for the HEU control element (not to scale).....	46
B4. The computational model for the LEU standard element (not to scale).....	47
B5. The computational model for the LEU irradiation fuel element (not to scale).....	48
C1. The LEU cores investigated using the 16 fuel plate element.....	50
C2. The LEU cores investigated using the 18 fuel plate element.....	51
D1. HEU core power peaking factors.....	54
D2. Proposed LEU core power peaking factors.....	55
D3. HEU core power distribution.....	56
D4. Proposed LEU core power distribution.....	57
D5. Measured relative thermal flux of the HEU UMRR.....	58
E1. Moderator density coefficient versus temperature for the HEU and proposed LEU cores.....	60
E2. Moderator temperature coefficient versus temperature for the HEU and proposed LEU cores.....	61
E3. Moderator coefficients versus temperature for the HEU core.....	62

LIST OF ILLUSTRATIONS

vi

	Page
1. (a) Current HEU and (b) proposed LEU core configurations.....	26
2. Computational models of (a) HEU standard element, (b) LEU control element (not to scale).....	27
3. Calculated and measured lateral thermal neutron flux profiles through row D of the HEU core.....	28
4. Total moderator coefficient for the HEU and LEU cores.....	29
5. Reactivity of the UMRR void tube at the HEU core periphery (C-3).....	30
6. Lateral thermal flux profile along centerline of irradiation fuel element in grid position E-5.....	31
B1. The HEU standard element from UMRR blueprints (shown with top handle).....	44
B2. The HEU control element from UMRR blueprints.....	45
B3. The computational model for the HEU control element (not to scale).....	46
B4. The computational model for the LEU standard element (not to scale).....	47
B5. The computational model for the LEU irradiation fuel element (not to scale).....	48
C1. The LEU cores investigated using the 16 fuel plate element.....	50
C2. The LEU cores investigated using the 18 fuel plate element.....	51
D1. HEU core power peaking factors.....	54
D2. Proposed LEU core power peaking factors.....	55
D3. HEU core power distribution.....	56
D4. Proposed LEU core power distribution.....	57
D5. Measured relative thermal flux of the HEU UMRR.....	58
E1. Moderator density coefficient versus temperature for the HEU and proposed LEU cores.....	60
E2. Moderator temperature coefficient versus temperature for the HEU and proposed LEU cores.....	61
E3. Moderator coefficients versus temperature for the HEU core.....	62

E4. Moderator coefficients versus temperature for the LEU core..... 63

E5. Doppler coefficient versus temperature for the
proposed LEU core..... 64

E6. Reactivity worth of a mid-core void versus percent voiding
of water for the HEU core..... 65

LIST OF TABLES

viii

	Page
I. Measured and calculated excess reactivities ($\beta\Delta k/k$) in the W and T modes for the HEU and proposed LEU cores.....	22
II. Reactivity coefficients calculated for the HEU and proposed LEU cores ($\beta\Delta k/k/^\circ C$).....	23
III. Measured and calculated void coefficient ($\beta\Delta k/k/cm^3$).....	24
IV. Reactivity worths of the Core Access element for the proposed LEU core ($\beta\Delta k/k$).....	25
B-I. Lattice spacing for the HEU and proposed LEU cores (cm).....	41
B-II. Number densities and volume fractions for the homogenized zones of the HEU and LEU cores.....	42
D-I. Power peaking factor definitions.....	52
F-I. Calculated and measured control rod worths for the UMRR HEU core ($\beta\Delta\Delta k/k$).....	68
F-II. Calculated and measured worth of the regulating rod in the HEU core ($\beta\Delta k/k$).....	69
G-I. Various irradiation fuel element designs, power peaking factors and thermal fluxes in grid position E-5.....	70
G-II. Raw data for CA experiment.....	71
G-III. Reactivity of CA element for normal (air-filled) and flooded conditions. Cases A and B are experimental data and 2L ^S -UM are from computer modeling ($\beta\Delta k/k$).....	71

NEUTRONICS STUDY OF THE CONVERSION
OF THE UNIVERSITY OF MISSOURI-ROLLA REACTOR
TO LOW ENRICHED URANIUM FUEL

by

Lorne J. Covington

University of Missouri-Rolla
Nuclear Engineering Department
Rolla, Missouri 65401

(314) 341-4236

ABSTRACT

The neutronics calculations for the conversion of the University of Missouri-Rolla Reactor (UMRR) from highly enriched uranium fuel (HEU) to low enriched uranium fuel (LEU) are studied. Several computational models of both the present HEU and proposed LEU cores are developed for two-dimensional neutron diffusion calculations using the 2DB-UM code. The core multiplication factors, neutron flux profiles, power peaking factors, moderator and void coefficients are calculated for both cores. The current HEU irradiation facilities are modeled and an irradiation fuel element for the LEU core is developed. Available experimental data for the HEU core are compared to computer results for a verification of the computational models.

Results show that the reactor conversion will not have any major adverse effect on the operation of the UMRR. The criticality should be reached with approximately the same number of LEU fuel and control elements as in the present HEU core. Power peaking factors for the LEU core are of the same magnitude as for the HEU core and are well below the limits established in the UMRR Safety Analysis Report. All reactivity coefficients remain negative.

1. INTRODUCTION

In the near future the high enriched uranium (HEU) fuel in the University of Missouri-Rolla Reactor (UMRR) will be replaced with low enriched uranium (LEU) fuel. The U. S. Nuclear Regulatory Commission requires a submittal of all necessary changes in the licensing documents before an order to convert can be issued. This paper presents the results of the neutronics study of such a fuel replacement. A concurrent independent study was performed by the Reduced Enrichment for Research and Test Reactor (RERTR) Program at the Argonne National Laboratory (ANL). The RERTR Program used a different set of computer codes to corroborate the analyses performed in this study.

The present HEU core consists of 14 fuel elements, 4 control elements and 1 half element. A standard fuel element consists of 10 curved fuel plates connected by two aluminum side plates. A control element consists of 6 curved fuel plates connected by two aluminum side plates with an aluminum guide tube for the control rod located in the center of the element. The half element is similar to the standard fuel element, except that five fueled plates in one half of the element are replaced with solid aluminum plates. The HEU fuel plate consists of aluminum cladding surrounding U_3O_8 -Al fuel enriched to 90% ^{235}U .

The LEU fuel material will be U_3Si_2 in an aluminum matrix with a ^{235}U enrichment of 19.75%. The standard fuel element contains 18 curved fueled plates connected by two aluminum sideplates. The control element is similar to the LEU standard element, except that 10 of the center plates are removed and an aluminum guide tube is inserted. The LEU half element is similar to the LEU standard element with 9 fueled plates replaced with aluminum plates in either half of the element.

The UMRR is a pool-type reactor presently licensed for 200 kW and is cooled by natural convection. The UMRR core is suspended from a movable bridge which allows operation in two different modes: a completely water reflected mode and a thermal column reflected mode in which one side of the reactor faces a graphite thermal column. The UMRR has one bare and one cadmium lined pneumatic tube facility and one beam port facility. The reactor control is accomplished by three oval borated steel shim/safety rods and one oval stainless steel regulating rod. The current HEU core and the proposed LEU core configuration, as developed within the course of this study, are shown in Figure 1.

$$D_E \nabla^2 \phi_E - \Sigma_{r,E} \phi_E + S_E = 0 \quad E=1 \text{ to } N \quad (1)$$

where the source term is defined as

$$S_E = \frac{\chi_E}{k_{\text{eff}}} \sum_{E'=1}^N (\nu \Sigma_f)_{E'} \phi_{E'} + \sum_{E'=1}^{E-1} (\Sigma_s)_{E' \rightarrow E} \phi_{E'} \quad (2)$$

The third dimension, which is in the axial direction, is handled by the input of an axial buckling term which is defined as:

$$(\pi / (\text{active fuel height} + 2 * \text{extrapolation length}))^2 \quad (3)$$

The axial extrapolation length was provided by ANL using a 3-D diffusion model of the UMRR (5). Two-energy group LEOPARD cross sections were input for the 2DB-UM calculations (hence $N=2$ in Eqs.(1) and (2)).

The standard element is divided into five homogenized zones: two side plate zones, two end plate zones and one zone for the interior fuel plates. The control element is divided into seven homogenized zones: two side plate, two fueled end plate, two interior fuel plate zones, and one zone containing the control rod guide tube and water channel. The pneumatic tubes were modeled by homogenizing all materials over the cell. The number densities were calculated for each material in each zone and then smeared over the volume of the cell. The fuel plates were assumed to be straight to simplify mesh generation in the diffusion code. Figure 2 shows the computational model of the HEU standard fuel element (a) and a proposed LEU control fuel element (b). The dashed lines show the division of the elements into the different homogenized zones.

A detailed computational mesh in the X-Y plane was then developed. The number of mesh lines per element was 10 in the X direction and 12 in the Y direction with an approximate spacing of 1 cm. The X-Y mesh

included very fine mesh lines at the edges of all fueled regions to allow for a determination of thermal flux peaking in the element.

III. REACTOR CALCULATIONS

The first phase of the neutronic calculations was performed for the present UMRR HEU core. The reactor geometry and materials were carefully modeled so that a comparison could be made with measured data.

III.A Effective Multiplication Factor and Thermal Flux Distribution

Using the procedure described above the effective multiplication factor, k_{eff} , was calculated for the HEU core in both the water reflected and the graphite reflected mode. The values are in good agreement with measured data and are shown in Table I.

The LEU core was then modeled following the same guidelines used in modeling of the HEU core. A problem in generating cross sections for the LEU fuel material U_3Si_2 was that silicon cross sections were unavailable in LEOPARD. A discussion with the RERTR Program staff determined that aluminum cross sections could be used in place of those of silicon [5]. Two different LEU element types and several different core configurations were developed. Both element types contained 18 plates with the difference being that one element type had all the plates fueled and the other had the two outer plates replaced with aluminum plates. The cores developed using the 18 fueled plate element contained approximately the same number of elements as the current HEU core and one core configuration was found which resembled the present core. It was, therefore, decided to pursue only this core configuration. Results of k_{eff} calculations for this core are shown in Table I.

Besides the computational mesh described in Section II, a second

mesh, called the fine mesh, was created for modeling the LEU irradiation fuel element. The difference between the two meshes is that row E had 20 mesh lines in the Y-direction in order to model individual fuel plates.

The 2DB-UM k_{eff} values for the LEU core are higher than the ANL results. The difference is attributed to the use of aluminum cross sections instead of those for silicon and to an uncertainty associated with the axial buckling term. This term was found to be a very sensitive parameter and could have been adjusted to produce a wide range of values for k_{eff} . The difference between the fine and coarse mesh values of k_{eff} is attributed to the fact that the row containing the fine mesh enables a more detailed description of thermal neutron flux in the core and reflector. The spacing of the fine mesh (0.1-0.4 cm) is on the order of the thermal diffusion coefficient for the reflector and fuel regions, 0.17 and 0.24 cm^{-1} , respectively. This is especially important when the neutron leakage (and return) term is calculated. The fast neutrons, which have leaked out of the core, are thermalized in the reflector and subsequently these neutrons then diffuse back into the core. It is this portion of the flux which is described better with the fine mesh model. A detail comparison of the two different meshes show a 6% increase in the number of thermal neutrons returning into the core. There is a similar effect seen in the other rows, but to a lesser extent. Overall, this effect manifests itself with an increase in the value of k_{eff} for the fine mesh.

The power peaking factor and power distribution were determined for each element position in the HEU and LEU core. The power peaking factor is defined to be the peak power in the element divided by the

average power in the core. Average power densities were obtained directly from 2DB-UM by selecting edits that perform averaging over requested zones. The peak thermal flux in the element was found by scanning 2DB-UM thermal flux outputs in the particular element for the maximum value and then determining the X-Y coordinates where that value occurred. The peak power density was then calculated by summing the product of flux and fission cross section for all energy groups at the determined X-Y coordinates.

The maximum power peaking factor for the HEU core as determined from the 2DB-UM and ANL calculations was 2.00 and 2.19, respectively. For the LEU core, the power peaking factors were 2.22 and 2.34, respectively. The element in which the maximum power peaking factor occurred was, in all cases, the control element C3. The increased value of the power peaking factor in the LEU case is still well within the power peaking limits of 3.0 to 4.0 prescribed in the UMRR Safety Analysis Report (6).

A comparison was made of the measured and calculated thermal flux distribution at the midplane of the HEU core. Figure 3 shows the lateral flux profile through row D compared with measured values of the thermal flux. The accuracy of the measured data within the core is about $\pm 30\%$. Outside the core the flux values are known with much less accuracy. The comparison shows that the calculated thermal flux distribution is slightly flatter across the core than the measured values, except the peak occurring in the control element. This flattening of the thermal flux was investigated and was determined to come from the use of the two-energy group cross sections. A sensitivity study was performed which consisted of varying the magnitude of fast

diffusion coefficient, D_1 in Eq. (1). Varying D_1 changes the fast leakage of the core, which causes a change in the fast and thermal flux shapes. The study showed that a slight decrease in the fast transport cross section and consequently an increase in D_1 caused the calculated thermal flux to better fit the measured data.

III.B Reactivity Coefficients

The moderator temperature, moderator density and total moderator reactivity coefficients were calculated for both the LEU and HEU cores. The Doppler coefficient was calculated only for the LEU core.

The procedure to calculate the reactivity coefficients consisted of generating sets of macroscopic cross sections for the fueled regions of the reactor with only one parameter affecting the reactivity changed at a time. These cross sections sets were then used as input for the global 2DB-UM problem to obtain values for k_{eff} from which the pertinent reactivity coefficient was determined. Cross sections for the Doppler coefficient were generated by changing only the resonance fuel temperature input data in LEOPARD in the range from 20 to 600 °C. The resonance fuel temperature is used by LEOPARD in the calculation of U^{238} resonance absorption in the epithermal energy range. Cross sections for the moderator density coefficient were generated in a similar manner, but only the moderator volume fraction was changed for each LEOPARD run. The volume fractions were calculated for water densities at temperatures from 20 to 100 °C. When calculating the moderator temperature coefficient cross sections, the only value that should be changed is the moderator temperature. In LEOPARD, however, a change of the moderator temperature causes the code to adjust the

moderator number density corresponding to the thermal expansion of the moderator. To negate this adjustment, the volume fraction (vf) of the water must be adjusted such that the number density used in calculating the macroscopic cross sections is the same as that for the base case. These adjusted volume fractions were determined by running LEOPARD at each selected moderator temperature using the base volume fraction and then calculating the adjusted volume fraction by taking the ratios of the hydrogen number density in the moderator N_H as follows:

$$(vf)_{\text{adjusted}} = \frac{(N_H)_{T = 20 \text{ } ^\circ\text{C}}}{(N_H)_{T \text{ selected}}} \quad (4)$$

The temperatures for the moderator temperature coefficient ranged from 20 to 100 °C. For the base case, the temperature of all materials was chosen to be 20 °C and the moderator volume fraction to be 1.0.

The calculated reactivity coefficients are tabulated in Table II. The results show that the total moderator coefficient, while still negative, is of smaller magnitude for the proposed LEU core than the HEU core. This was to be expected because the greater number of plates in the proposed LEU core reduces the amount of moderator in the core. The Doppler coefficient for the LEU core is also negative, but is an order of magnitude smaller than the total moderator coefficient for the operating range of the reactor.

Figure 4 shows the calculated total moderator coefficient for the HEU and LEU cores along with the measured moderator coefficient for the HEU core. The measured total moderator coefficient is shown only for the normal operating range of the reactor. It shows a good agreement between the measured and the calculated HEU value for low temperature. However, one should note, that the calculated value slightly

overpredicts the measured value.

The void coefficient was calculated for a midcore position (E-5) and a peripheral position (C-7 in the HEU and C-3 in the LEU core). Two different approaches were used to model a void. The first approach was to slowly decrease the water number density in the void region and calculate k_{eff} in corresponding 2DB-UM runs. For both the midcore and peripheral calculations, this lead to increasing instabilities as the percent voiding of the region approached 100%. A strong non-linear relationship between the reactivity and voided fraction was also observed.

The second approach was developed in that air was replaced by aluminum whose cross sections were modified (7). A base set of macroscopic aluminum cross sections was produced from LEOPARD. In each energy group the absorption cross section was reduced by a factor of 10^{-3} . The difference between the new absorption cross section and the base absorption cross section was then subtracted from the transport cross section. No changes were made to the scattering cross sections. The modified cross sections were then used as cross sections for air in the 2DB-UM global calculations.

Results of both methods along with a measured void are shown in Figure 5 for the HEU peripheral calculations. It shows that using the method of adjusted aluminum cross section yields the result which is close to a measured value of the peripheral void coefficient. This method was also stable during the calculation. This method was therefore used to calculate the void coefficient of the LEU core. The results of this calculation are shown in Table III together with the results for the HEU core.

III.C Irradiation Facilities and Control Rods

With the current 10 plate HEU fuel element, irradiations can be made using stringers suspended in between individual fuel plates. It is desirable to have a variation of this feature in the LEU core. The proposed 18 plate LEU fuel element will have limited access to the interior of the element. Therefore, an irradiation fuel (IF) element was designed. The areas of concern in the design of the IF element are maximization of the space used for irradiation, physical protection of the IF and minimization of the thermal load in the IF caused by thermal neutron flux peaking.

The geometry of the IF element is the same as the LEU standard fuel element except that a number of fuel plates were removed from one half of the IF element. In addition to simply removing fuel plates, two aluminum plates were inserted in the outermost positions from which the fuel plates were removed. These aluminum plates are inserted to protect the fueled plates on either side of the water channel from any damage that could potentially occur during insertion or removal of samples from the IF during operation.

Several different combinations of removed fuel plates and inserted aluminum plates were investigated for the IF element placed in the grid plate position E-5 of the LEU core. The combinations included runs with the removal of 2,4,6 and 8 fueled plates and runs with the removal of 4,6,8 and 10 fueled plates and the insertion of two aluminum plates.

The design of the IF element selected by the reactor staff was element with 8 fueled plates removed and 2 aluminum plates inserted. This design gives the maximum working area while not imposing any extreme thermal loads within the element. Figure 6 shows the centerline

geometry of the proposed IF element and the shape of the thermal neutron flux across the element. There is, by a factor of 1.5, an increased value of the thermal flux in the IF element as compared to the current HEU bare pneumatic tube facility.

The calculations have shown that the maximum and average thermal neutron flux in the water gap increased with the removal of each pair of fueled plates. The insertion of the aluminum plates did not appreciably lower the magnitude of the thermal neutron flux. The maximum power peaking factor for the least favorable position of the IF element (E-5) is very comparable to the maximum power peaking factor determined for the base LEU core design. The respective values are 2.31 in the IF element and 2.22 in the control rod element C3. Both of these power peaking factors are well within the thermal limits of the UMRR. The value of k_{eff} for the LEU core with this IF element design is 0.9873, therefore additional elements will have to be added to achieve criticality.

The core access (CA) element is a non-fueled element, made of aluminum and graphite. It is clad with an aluminum jacket which has two opposite sides curved to the same curvature as a fuel element. The interior of the element contains a piece of graphite with a circular center channel. The computational model of the CA used straight sides for the curved exterior sides and a square center channel. The CA element can be used either in a core periphery position or in the interior of the reactor core.

The reactivity worth of the CA element in the periphery position C-7 of the HEU core was determined experimentally and by a 2DB-UM calculation. Two different cases were investigated. The first case was

with the center channel containing air, which is the normal mode of operation. The second case was with the center channel flooded with water. To simulate air in the center channel of the CA element, the method developed for the calculation of the void coefficient was used.

There is a good agreement between the measured reactivity, 0.425%, and calculated reactivity, 0.479%, for the flooded CA element in the HEU periphery. The measured reactivity worth of replacing the water with air is -0.161%, while the calculated worth is -0.058%.

The CA element was modeled for two reactor positions in the LEU core: the peripheral position C-3 and the midcore position E-5. The reactivity worth of the CA element in the periphery position was calculated to be -0.142%. Flooding of the CA element had a worth of -0.112%. The midcore calculation showed the worth of the air to be 0.517%. Results of the calculations for the CA element in the flooded condition are summarized in Table IV.

The important consideration is that negative reactivity is added to the reactor for all cases in which the CA element goes from the normal air-filled operation to abnormal flooded operation.

Control rods for the UMRR are solid stainless steel 304 (SS 304) with boron added to increase neutron absorption. Such strongly absorbing control rods can not be modeled directly using LEOPARD and 2DB-UM. Indirect modeling can be performed by using a reaction rate matching method.

The reaction rate matching method consists of using a Monte Carlo code to determine the ratio of the absorption rate in the control rod/guide tube region to the fission rate in a unit cell. This ratio is then matched in a 2DB-UM calculation by adjusting the control rod

absorption cross sections. The unit cell, for which the calculation is performed, consists of a control element surrounded by 8 standard fuel elements with reflected boundary conditions on all four sides (8).

Monte Carlo calculations were performed by the RERTR group and the data provided to us (5). When the reaction rate method was applied to the HEU core, the calculated reactivity worths were nearly identical for all shim/safety control rods. Their measured worths, however, vary greatly depending on their core position. This led to the conclusion that the unit cell model cannot be used for the small core of the UMRR. Rather the whole core with all shim safety rods present would have to be modeled and the reaction rates for each rod adjusted simultaneously. This, however, was judged as being beyond the scope of the work and was not attempted for either the HEU or LEU core.

The regulating rod for the UMRR is a SS 304 tube. It is considered to be a weak absorber and therefore was modeled using LEOPARD and 2DB-UM directly. The SS 304 is homogenized across the entire guide tube region and the resulting cross sections used in a global 2DB-UM calculation. The calculated worth of -0.31% agrees well with the measured worth of -0.35% for the HEU core.

IV. CONCLUSIONS

The results of this study show that a conversion to the LEU core will not have adverse effects on the operation of the UMRR. The criticality of the new core will be reached with approximately the same number of fuel elements and in a similar configuration as the HEU core. Power peaking factors are only slightly larger for the LEU core, but are still well within the requirements of the thermal hydraulics analysis. The moderator temperature coefficient is about 40% smaller than for the HEU core. The moderator temperature coefficient and Doppler coefficient provide the desirable negative reactivity feedback with increasing temperature. The irradiation fuel element in the LEU core will improve the UMRR irradiation capabilities by providing a thermal flux twice the magnitude previously obtained in the HEU core.

The codes used in the study, LEOPARD and 2DB-UM, provided adequate results for most cases. They were easy to set up, run and likewise their input was simple. Their convergence and run times were short. A disadvantage of LEOPARD is that it only provided two-energy or four-energy group cross section sets. It is believed that a larger number of energy groups would have provided better results during the calculations of the moderator and void coefficients. The main limitation of the two-dimensional model was in determining the value of the axial buckling term. The best assumption that could be made was choosing a chopped cosine representation of the axial flux distribution. Experimental data show that this definitely was not the case. The large aluminum grid plate at the bottom of the core and strongly absorbing control rods present at the top of the core contribute to the deformation of the flux shape.

Future work could be better performed using a 3-D diffusion code and a cross section collapsing code that is more flexible with respect to energy group structure.

ACKNOWLEDGEMENT

This study was supported by the U.S. Department of Energy under Grant No. DE-FG02-86ER75272.

NOMENCLATURE

- D - diffusion coefficient
- g or g' - subscript denoting energy group
- k_{eff} - effective multiplication factor
- N_H - hydrogen number density
- S - neutron source
- T - temperature
- Greek
- ν - average number of neutrons released per fission
- Σ_r - macroscopic removal cross section
- Σ_f - macroscopic fission cross section
- $\Sigma_{s,g' \rightarrow g}$ - macroscopic scattering cross section from energy group g' to energy group g
- χ_g - probability that a fission neutron will be born in energy group g
- ϕ - neutron flux

REFERENCES

1. R. F. Barry., "LEOPARD - A Spectrum Dependent Non-spatial Depletion Code for the IBM-7094", Westinghouse Electric Corporation, WCAP-3269-26, 1963.
2. "Leopard Manual", Argonne National Laboratory, RERTR group, May 1981.
3. W. W. Little, Jr. and R. W. Hardie., "2DB Users Manual - Revision 1", Battelle Memorial Institute, BNWL-831 REV1, 1969.
4. "2DB-UM Users Manual", Argonne National Laboratory, RERTR group, May 1980.
5. J. Matos, Personal Communication, Argonne National Laboratory, RERTR group, Summer 1986.
6. Safety Analysis Report, University of Missouri-Rolla Reactor Facility, License number R-79, Sept. 1984.
7. J. Matos, Personal Communication, Argonne National Laboratory, RERTR group, February 1987.
8. L. J. Covington. "Neutronics Study of the Conversion of the University of Missouri-Rolla Reactor to Low Enriched Uranium Fuel", MS Thesis, University of Missouri-Rolla, 1989.

TABLE I

Measured and calculated excess reactivities in the W and T modes for the HEU and proposed LEU cores ($\beta\Delta k/k$).

HEU Core	W-mode	T-mode
Measured	0.27-0.35	0.73-0.80
Calculated (this work)	0.21	0.57
Calculated (ANL)	0.23	0.48
LEU Core	W-mode	T-mode
Calculated (this work)	0.81	1.19
	1.22*	1.52*
Calculated (ANL)	0.17	n/a

* very fine mesh in row E

TABLE II

Reactivity coefficients calculated for the HEU and proposed LEU cores ($\Delta k/k/^\circ\text{C}$).

Coefficient		UMR	ANL
moderator (20-50 °C) total (50-100 °C)	HEU	-0.0210	-0.0141
	LEU	-0.0135	-0.0121
	HEU	-0.0262	-0.0186
	LEU	-0.0183	-0.0167
Doppler	LEU	-0.00108	-0.00176

TABLE III

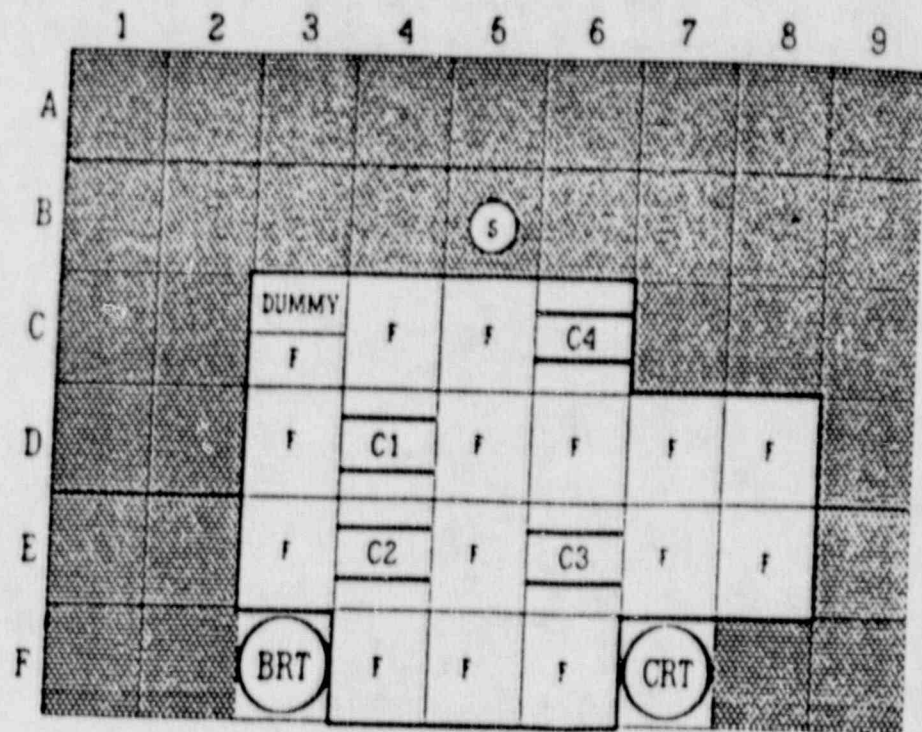
Measured and calculated void coefficient ($\Delta k/k/cm^3$).

Core	Periphery	Midcore
HEU measured	-1.10E-04	n/a
HEU calculated	-6.68E-05	2.36E-04
LEU calculated	-9.03E-05	3.26E-04

TABLE IV

Reactivity worths of Core Access element for
the proposed LEU core ($\beta\Delta k/k$).

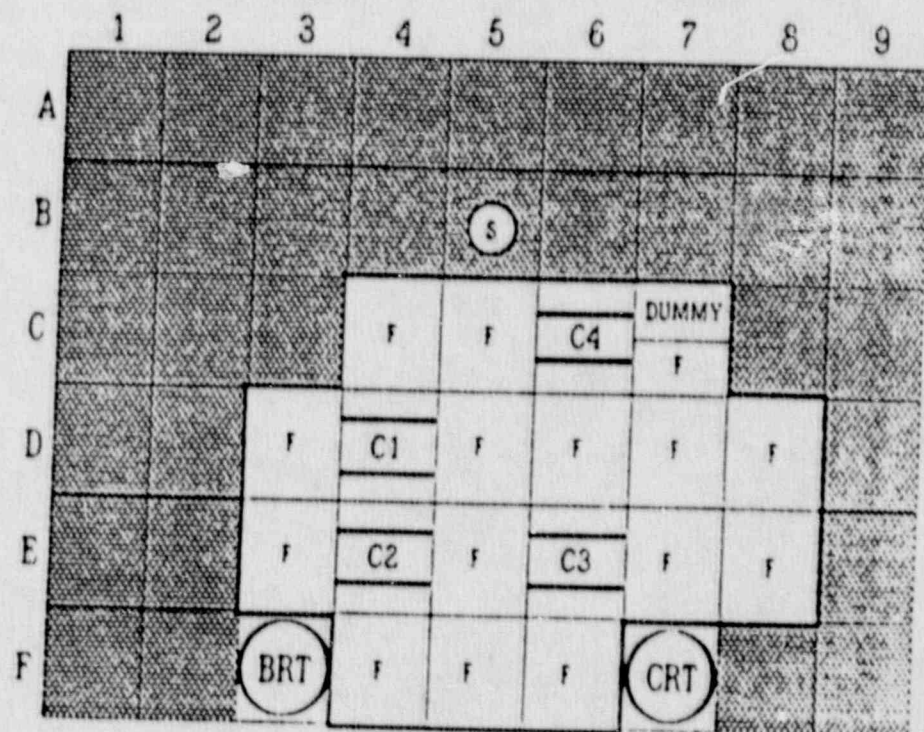
	Periphery	Mid-core
CA with air	-0.030	-4.501
CA with water	-0.142	-5.018



(a)

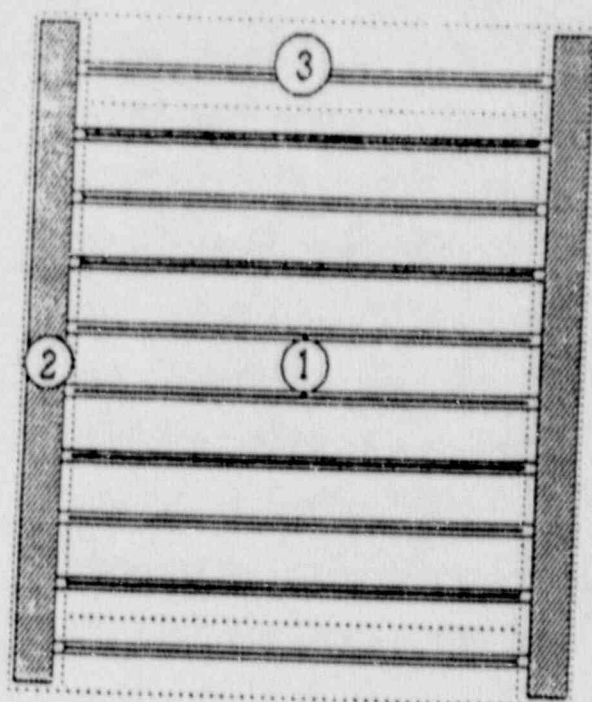
F - standard fuel element
 S - source tube
 C1 - C4 - control fuel element

BRT - Bare rabbit tube
 CRT - Cadmium rabbit tube



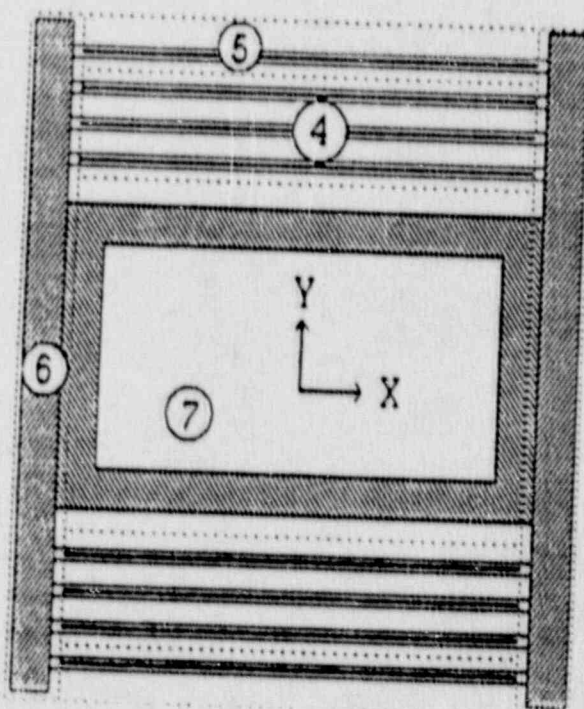
(b)

FIG. 1. (a) Current HEU and (b) proposed LEU core configurations.



- 1 - HEU interior fuel, clad and moderator zone
- 2 - Standard element side plate
- 3 - Standard element end plate

(a)



- 4 - LEU interior fuel, clad and moderator zone
- 5 - Control element end plate
- 6 - Control element side plate
- 7 - Guide tube and water region

(b)

Fig. 2. Computational models of (a) HEU standard element, (b) LEU control element (not to scale).

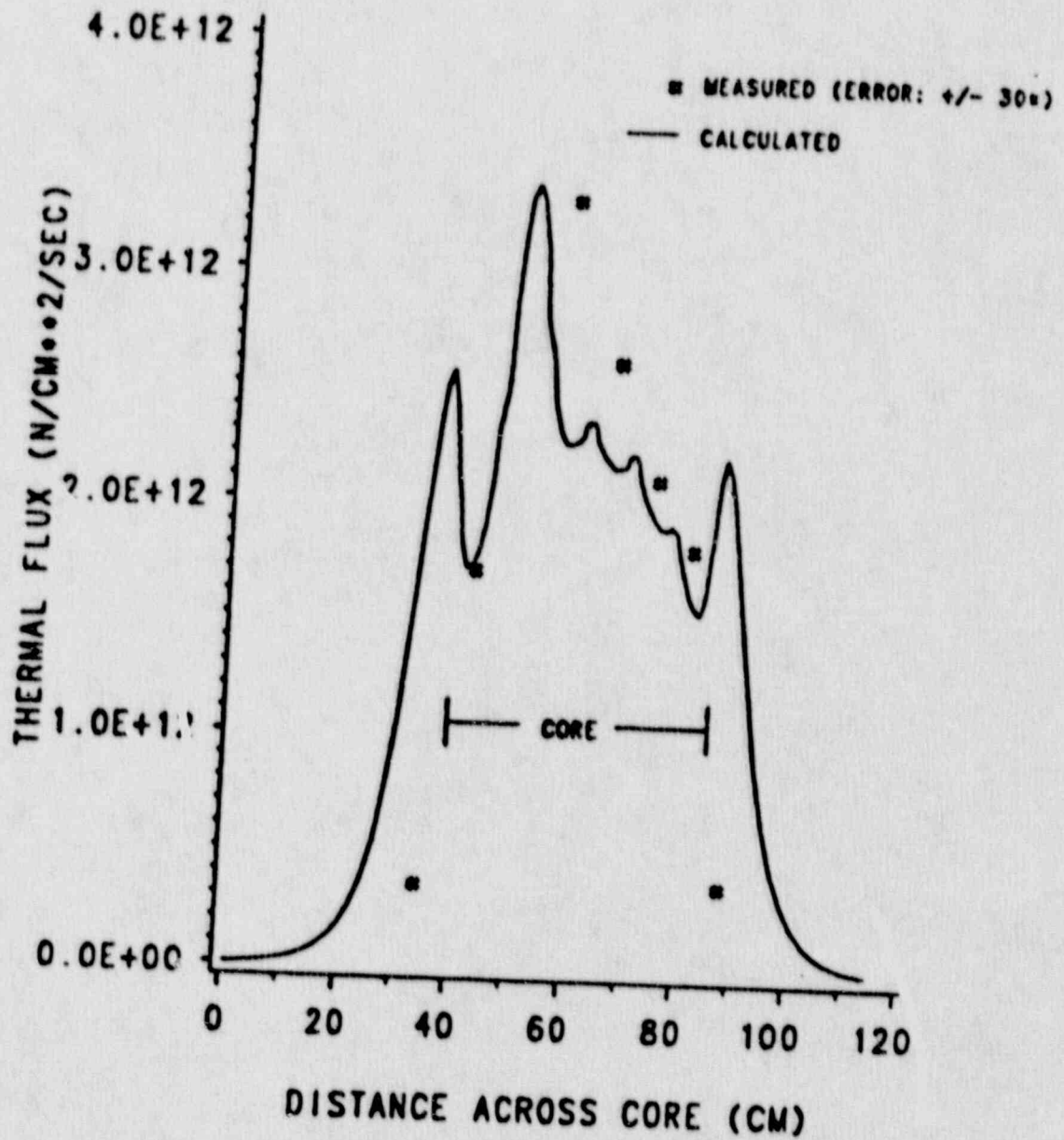


Fig. 3. Calculated and measured lateral thermal flux profiles through row D of the HEU core.

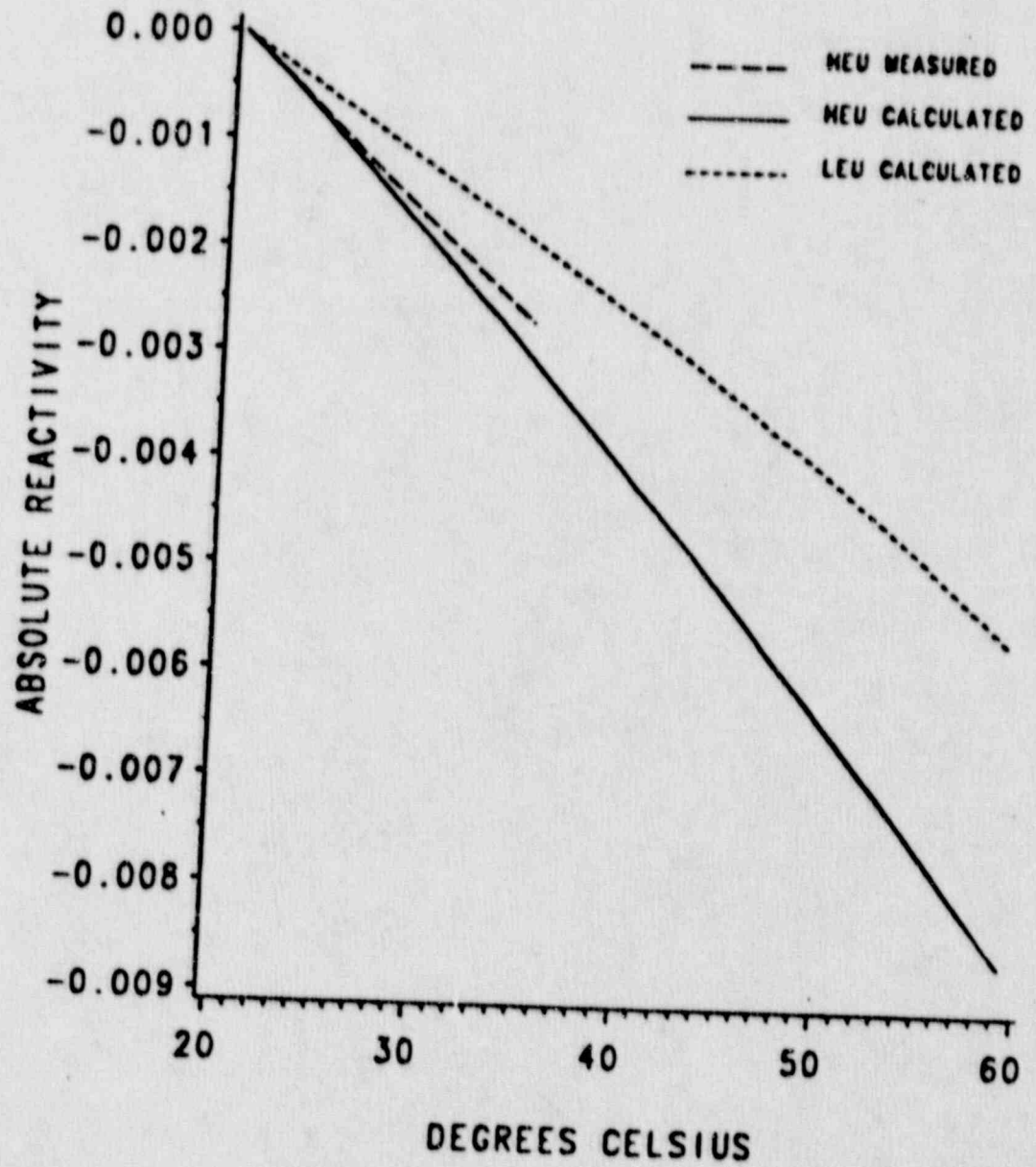


Fig. 4. Total moderator coefficient for the HEU and LEU cores.

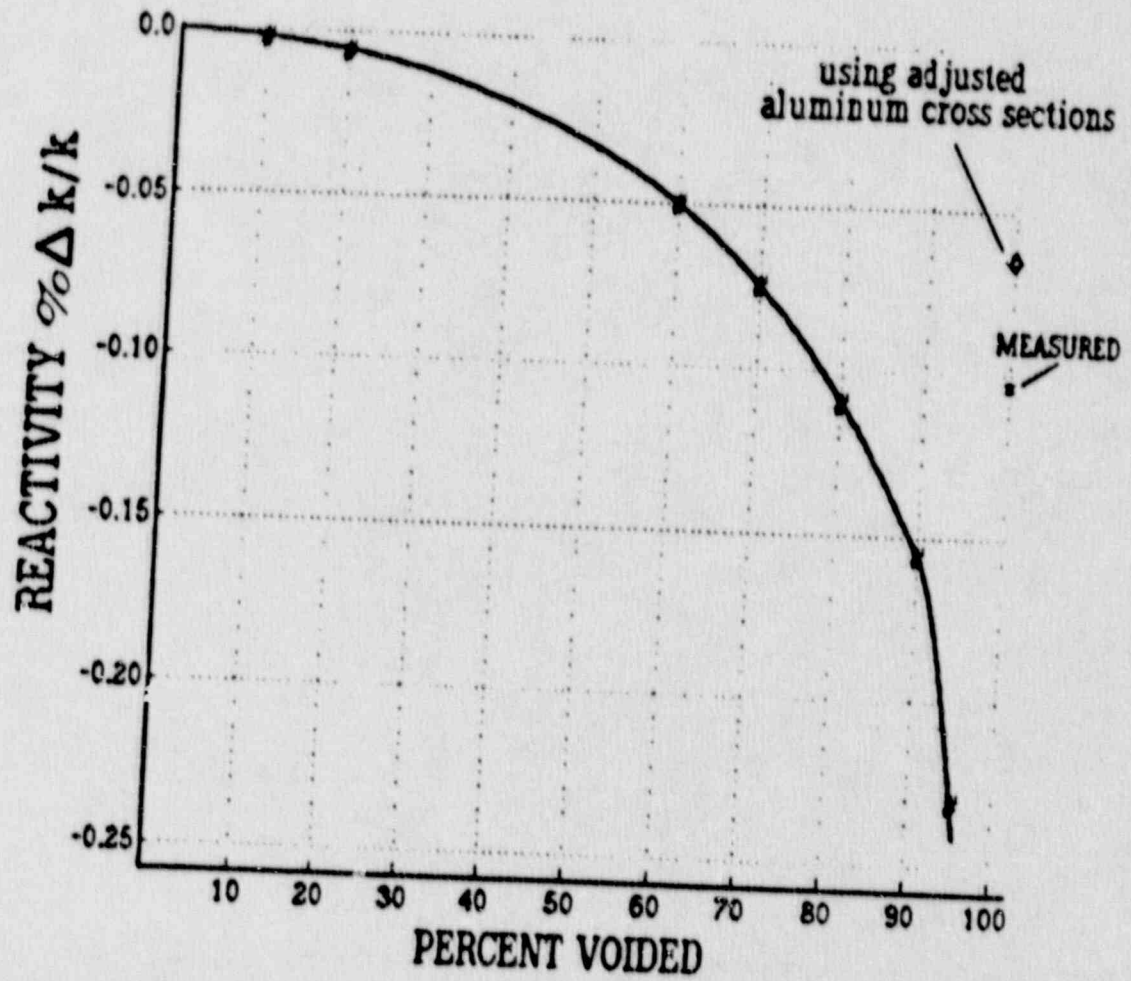


Fig. 5. Reactivity of the UMRR void tube at the HEU core periphery (C-3).

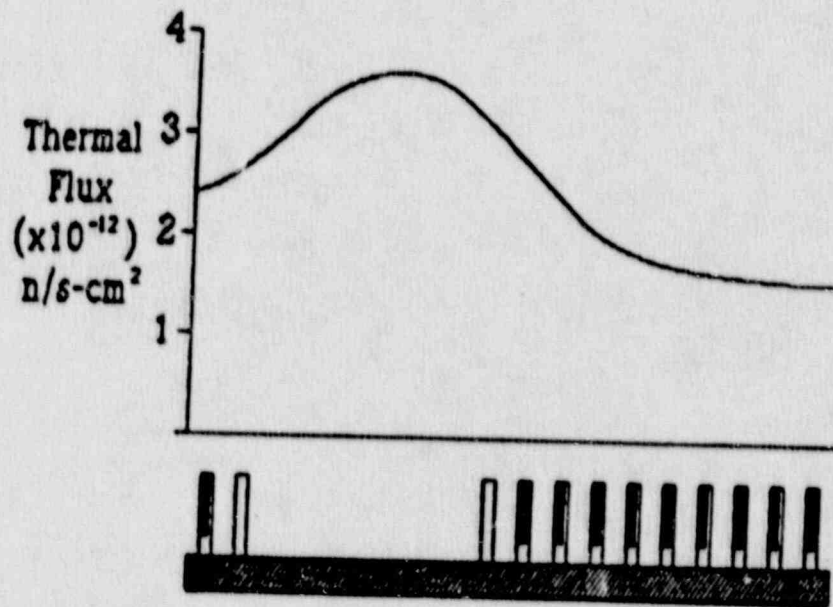


Fig. 6. Lateral thermal flux profile along centerline of irradiation fuel element in grid position E-5.

ADDITIONAL REFERENCES

9. RERTR Program Report, "Properties of Fuel Meat Materials", Argonne National Laboratories RERTR.
10. G. L. Copeland and others, "Performance of Low-Enriched U_3Si_2 Aluminum Dispersion Fuel Elements in the Oak Ridge Research Reactor", Argonne National Laboratory, July 1987.
11. M. M. Bretscher, "Blackness Coefficients, Effective Diffusion Parameters and Control Rod Worths for Thermal Reactors", Argonne National Laboratory, ANL/RERTR/TH-5, 1984.
12. J. L. Snelgrove, "Method for Computing Axial Extrapolation Lengths", Argonne National Laboratory, 1984.
13. "Research Reactor Core Conversion from the Use of Highly Enriched Uranium to the Use of Low Enriched Uranium Fuels Guidebook", International Atomic Energy Agency, Vienna, Austria, 1980.

VITA

Lorne Joseph Covington was born January 20, 1963 in Normandy, Missouri. He received his elementary education in Denver, Colorado and St. Louis, Missouri. He received his high school education at Riverview Gardens High School in St. Louis, Missouri. He is married with no children.

He entered the University of Missouri-Rolla, Rolla, Missouri in August 1981. He received his B.S. in Nuclear Engineering from the University of Missouri-Rolla in May 1986.

He entered the Graduate School of the University of Missouri-Rolla in August 1986 as a candidate for the degree of Master of Science of Nuclear Engineering.

APPENDIX A
CODE DESCRIPTIONS AND INPUT EXAMPLES

A1. LEOPARD

LEOPARD is a zero-dimensional cross section collapsing code using a MUFT-SOFOCATE model of the neutron spectrum. The code was developed by R.F. Barry of the Westinghouse Electric Corporation in 1963. The code assumes a regular lattice of fuel, clad and moderator. An "extra" region is included to develop cross sections for non-fueled regions such as guide tubes, sideplates, graphite reflector, etc. The thermal spectrum is modeled with a Wigner-Wilkins spectrum at 172 energy points from 0 to 0.625 eV. The fast spectrum uses a consistent B-1 MUFT-IV spectrum. The cross section library consists of isotopes commonly used in light water reactor analysis.

Input for LEOPARD is broken into 3 groups: input flags, lattice geometry and material compositions. The lattice geometry is divided into a fuel material region, a clad and void region, a moderator region and the "extra" region. For the plate type fuel used in this study, the region thicknesses were measured from the center of the plate to the center of the water channel. Material compositions are inputted in two different ways depending on the isotope described. Trace elements such as ^{235}U , ^{238}U , and ^{10}B are inputted with number densities in $\#/barn/cm$. Other materials such as H_2O , aluminum, graphite, SS 304, are inputted by their volume fraction in the homogenized zones.

On the following page, the JCL and input data for running a sample LEOPARD problem are given.

```

//L11 JOB (0368\Slb.####), 'COVINGTON, LORNE', MSGLEVEL=(1,1), TIME=1,
//      MSGCLASS=8
//S1 EXEC PGM=LEOPARD
//STEPLIB DD DSN=USER.X0368.LEOPARD.1MOD, DISP=SHR
//GO.FT01F001 DD DSN=USER.X2903.LEOPARD.1LIBIN2, DISP=SHR
//* LEOPARD ENDF/B-IV DATA LIBRARY FILE
//GO.FT03F001 DD DSN=&WRESTRT, UNIT=SYSDA, SPACE=(TRK,(3,1)),
//      DISP=(,DELETE), DCB=(RECFM=VBS, LRECL=X, BLKSIZE=6136)
//* RESTART FILE WRITTEN BY LEOPARD - OUTPUT
//GO.FT04F001 DD DSN=&RRESTRT, UNIT=SYSDA, SPACE=(TRK,(3,1)),
//      DISP=(,DELETE), DCB=(RECFM=VBS, LRECL=X, BLKSIZE=6136)
//* RESTART FILE READ BY LEOPARD - INPUT FOR RESTART
//GO.FT06F001 DD SYSOUT=W
//GO.FT07F001 DD DSN=&LINUX, UNIT=SYSDA, SPACE=(TRK,(5,1)), DISP=(,DELETE),
//      DCB=(RECFM=VBS, LRECL=X, BLKSIZE=6136)
//* BINARY FILE OF CROSS-SECTION DATA FOR LINUX CODE - BURNUP DEPENDENT
//GO.FT08F001 DD SYSOUT=V
//* FORMATED FILE OF CROSS-SECTIONS FOR 2DBUM CODE
//GO.FT10F001 DD DSN=&ENER, UNIT=SYSDA, SPACE=(TRK,(2,1)),
//      DISP=(,DELETE), DCB=(RECFM=VBS, LRECL=X, BLKSIZE=6136)
//* ENERGY AND TEMPERATURE DATA
//GO.FT16F001 DD DSN=&SPECTRM, UNIT=SYSDA, SPACE=(TRK,(2,1)),
//      DISP=(,DELETE), DCB=(RECFM=VBS, LRECL=X, BLKSIZE=6136)
//* SPECTRUM DATA
//GO.FT20F001 DD DSN=&MICROXS, UNIT=SYSDA, SPACE=(TRK,(5,1)),
//      DISP=(,DELETE), DCB=(RECFM=VBS, LRECL=X, BLKSIZE=6136)
//* MICRSCOPIC CROSS-SECTION DATA BY BURN STEP
//GO.FT05F001 DD *

```

```

                HEU CORE
1 0 0 2 1 0 0 0 0 0 1
      9      0.9037      1.0077      0.0      1.0077
      2      6.6680E-3
      18     2.2540E-3
      20     2.4720E-4
      100      0.0      0.0      1.000      0.0000
      777
      777
      70.0      70.0      70.0      70.0      0.010
0.0254      0.0762      0.8103      1.0      0.0      0.5
      25.6

```

```

/*
//

```

A2. 2DB-UM

2DB-UM is a two-dimensional, multigroup diffusion code. 2DB-UM is a modification of the 2DB code developed in 1969 by Little and Hardie of Battelle Laboratory in Richland, WA. The modifications were made at the University of Michigan and included the addition of FIDO, the free format input processor, edit capabilities, improved calculational methods and additional input options. Version #6, 1980 of 2DB-UM was used in this study.

2DB-UM solves the multigroup diffusion in the following form:

$$D_g \nabla^2 \phi_g - \Sigma_{r,g} \phi_g + S_g = 0 \quad g=1,N \quad (A-1)$$

where

$$S_g = \frac{\chi_g}{k_{\text{eff}}} \sum_{g'=1}^N (v\Sigma_f)_{g'} \phi_{g'} + \sum_{g'=1}^{g-1} (\Sigma_s)_{g' \rightarrow g} \phi_{g'} \quad (A-2)$$

The difference equations are applied with placing the mesh point placed at the center of a homogeneous mesh interval. Boundary conditions used in this study were zero flux and zero flux gradient at the boundary.

Input consists of a set of input flags, description of the X-Y mesh, assigning to each mesh interval a zone number, associating a material for each zone and input macroscopic cross sections. Listed is JCL and input data for an example run of 2DB-UM.

```
//HAP JOB (0368VS1B,####), 'COVINGTON, LORNE', TIME=30,
//      MSGLEVEL=(1,1),MSGCLASS=W
//S1 EXEC PGM=UM2DB
//STEPLIB DD DSN=USER.X0368.UM2DB.LMOD,DISP=SHR
//GO.FT06F001 DD SYSOUT=W,DCB=(RECFM=FBA,LRECL=133,BLKSIZE=1596),
//      OUTLIM=20000
//GO.FT04F001 DD DSN=&SCRATCH,UNIT=SYSDA,SPACE=(CYL,(1,1)),
//      DISP=(,DELETE),DCB=(RECFM=VBS,LRECL=X,BLKSIZE=6136)
//* SCRATCH FILE FOR UM2DB DATA
//GO.FT08F001 DD DSN=&FLUXOUT,UNIT=SYSDA,SPACE=(CYL,(1,1)),
//      DISP=(,DELETE),DCB=(RECFM=VBS,LRECL=X,BLKSIZE=6136)
//* FLUX OUTPUT FILE - READ AND WRITTEN BY UM2DB
//GO.FT09F001 DD DSN=&SOURCE,UNIT=SYSDA,SPACE=(CYL,(1,1)),
//      DISP=(,DELETE),DCB=(RECFM=VBS,LRECL=X,BLKSIZE=6136)
//* SOURCE WRITTEN BY UM2DB
//GO.FT10F001 DD DSN=&XSECDMP,UNIT=SYSDA,SPACE=(TRK,(3,1)),
//      DISP=(,DELETE),DCB=(RECFM=VBS,LRECL=X,BLKSIZE=6136)
//* BINARY FILE OF CROSS-SECTION DATA FOR PERTV
//GO.FT14F001 DD DSN=&FLUXIN,UNIT=SYSDA,SPACE=(CYL,(1,1)),
//      DISP=(,DELETE),DCB=(RECFM=VBS,LRECL=X,BLKSIZE=6136)
//* INPUT FLUX GUESS FOR UM2DB CODE
//GO.FT15F001 DD DSN=&XSEGIN,UNIT=SYSDA,SPACE=(TRK,(2,1)),
//      DISP=(,DELETE),DCB=(RECFM=VBS,LRECL=X,BLKSIZE=6136)
//* INPUT CROSS-SECTION LIBRARY FOR UM2DB
//GO.FT17F001 DD DSN=&XSBRND,UNIT=SYSDA,SPACE=(TRK,(2,1)),
//      DISP=(,DELETE),DCB=(RECFM=VBS,LRECL=X,BLKSIZE=6136)
//* MATERIAL BURNUP DATA
//GO.FT18F001 DD DUMMY
//* FLUX PLOTTING DATA - OUTPUT FILE
//GO.FT19F001 DD DSN=&FLXSCR,UNIT=SYSDA,SPACE=(CYL,(3,1)),
//      DISP=(,DELETE),DCB=(RECFM=VBS,LRECL=X,BLKSIZE=6136)
//* FLUX COEFFICIENT SCRATCH DATA FILE FOR ARRAYS CXS, CXR, AND CXT
//GO.FT05F001 DD *
100 C WATER DENSITY **HEU CORE MODER TEMP COEFF.
```

-----1\$\$ ARRAY INTEGER CONTROL PARAMETERS-----

1\$\$

IREGAD	IEVTYP	ISERCH	NGPS	NXDOWN	NXCARD	NXTAPE	IGUESS
0	1	0	2	1	15	00	0
MOUTER	MINNER	IALDIR	IOVLAY	IGEOM	IM	JM	NZONES
100	5	0	0	0	98	71	58
NMAT	NMIXCD	IBCL	IBCR	IBCT	IBCB	NIZDEL	NJZDEL
15	0	0	0	0	0	0	0
NPRT	NOTUSED	NOTUSED	IXSTRT	IXEMIC	IEDIT	IGPBK	IDUP17 E
0	0	0	00	0	3	0	0 E

-----2** ARRAY REAL CONTROL PARAMETERS-----

2**

EV	EVM	PAREV	BUCK	ALAL	ALAH	EPS	EPSPAR
1.0	0.0	0.0	1.71000-3	0.0	0.0	5.0-4	0.0
EPSFLX	POD	ORF	POWER	FISMEV	XMWFA	ORFFS	ABLYVO E T
1.0-3	0.0	1.55	-3.281-3	193.1	0.0	1.0-5	590.16 E T

-----23** ARRAY X MESH INCREMENTS-(IM)-----

23**

1.628 1.27 4.127 2.54 1.264 2.54 2.051 10R1.925 4R0.9638
 0.6765 0.1 6R1.0262 0.1 0.6765 5Q10
 4R0.9638 6R1.925 2.051 2.54 1.264 2.54 4.127 1.27 1.628

-----24** ARRAY Y MESH INCREMENTS-(JM)-----

24**

3R4.05 3.589 2R1.27 9R2.54 2R1.27 5R0.9843 0.1 0.5726 5R1.351 0.57261
 2R0.1 0.5726 1.66 0.1 2R1.617 0.1 1.66 0.5726 0.1 2Q10 4R1.025
 2R2.025 4R4.05

-----5\$\$ ARRAY ZONE NUMBER FOR EACH MESH-(IM X JM)-----

5\$\$

1 32 94R34 32 1 3Q98
 1 3R32 90R34 3R32 1
 3R1 32 90R34 32 3R1 5Q98
 3R1 3R32 86R33 3R32 3R1
 5R1 32 86R33 32 5R1 2Q98
 5R1 88R32 5R1 1Q98
 31R1 10R29 10R30 10R31 37R1 4Q98
 21R1 10R35 2 8R38 2 2 8R39 2 2 8R40 2 10R36 27R1
 21R1 10R35 2 38 6R26 38 2 2 39 6R27 39 2 2 40 6R28 40 2 10R36 27R1 6Q98
 21R1 10R35 2 8R38 2 2 8R39 2 2 8R40 2 10R36 27R1
 21R1 2 8R41 2 37 8R42 37 2 8R43 2 37 8R44 37 2 8R45 2 2 8R46 2 17R1
 21R1 2 41 6R18 41 2 37 42 6R19 42 37 2 43 6R21 43 2
 37 44 6R22 44 37 2 45 6R24 45 2 2 46 6R25 46 2 17R1 1Q98
 21R1 2 41 6R18 41 2 37 8R42 37 2 43 6R21 43 2 37 8R44 37
 2 45 6R24 45 2 2 46 6R25 46 2 17R1
 16R1 1 3R1 1 2 41 6R18 41 2 37 8R20 37 2 43 6R21 43 2 37 8R23 37
 2 45 6R24 45 2 2 46 6R25 46 2 17R1 1Q98
 21R1 2 41 6R18 41 2 37 8R42 37 2 43 6R21 43 2 37 8R44 37
 2 45 6R24 45 2 2 46 6R25 46 2 17R1
 21R1 2 41 6R18 41 2 37 42 6R19 42 37 2 43 6R58 43 2
 37 44 6R22 44 37 2 45 6R24 45 2 2 46 6R25 46 2 17R1 1Q98
 21R1 2 8R41 2 37 8R42 37 2 8R43 2 37 8R44 37 2 8R45 2 2 8R46 2 17R1
 21R1 2 8R47 2 37 8R48 37 2 8R49 2 2 8R50 2 2 8R51 2 2 8R52 2 17R1
 21R1 2 47 6R10 47 2 37 48 6R13 48 37 2 49 6R14 49 2
 2 50 6R15 50 2 2 51 6R16 51 2 2 52 6R17 52 2 17R1 1Q98
 21R1 2 47 6R10 47 2 37 8R48 37 2 49 6R14 49 2
 2 50 6R15 50 2 2 51 6R16 51 2 2 52 6R17 52 2 17R1
 21R1 2 47 6R10 47 2 37 8R12 37 2 49 6R14 49 2
 2 50 6R15 50 2 2 51 6R16 51 2 2 52 6R17 52 2 17R1 1Q98
 21R1 2 47 6R10 47 2 37 8R48 37 2 49 6R14 49 2
 2 50 6R15 50 2 2 51 6R16 51 2 2 52 6R17 52 2 17R1
 21R1 2 47 6R10 47 2 37 48 6R13 48 37 2 49 6R14 49 2
 2 50 6R15 50 2 2 51 6R16 51 2 2 52 6R17 52 2 17R1 1Q98
 21R1 2 8R47 2 37 8R48 37 2 8R49 2 2 8R50 2 2 8R51 2 2 8R52 2 17R1
 21R1 2 8R53 2 2 8R54 2 2 8R55 2 37 8R56 37 2 8R55 2 27R1
 21R1 2 53 6R5 53 2 2 54 6R6 54 2 2 55 6R7 55 2 37 56 6R8 56 37
 1 1 6R1 1 1 27R1 1Q98
 21R1 2 53 6R5 53 2 2 54 6R6 54 2 2 55 6R7 55 2 37 8R56 37 1 8R1 1 27R1
 21R1 2 53 6R5 53 2 2 54 6R6 54 2 2 55 6R7 55 2 37 8R09 37 1 8R1 1 27R1
 21R1 2 57 6R4 57 2 2 54 6R6 54 2 2 55 6R7 55 2 37 8R09 37 1 8R1 1 27R1
 21R1 2 57 6R4 57 2 2 54 6R6 54 2 2 55 6R7 55 2 37 8R56 37 1 8R1 1 27R1
 21R1 2 57 6R4 57 2 2 54 6R6 54 2 2 55 6R7 55 2 37 56 6R8 56 37
 1 8R1 1 27R1 1Q98
 21R1 2 8R57 2 2 8R54 2 2 8R55 2 37 8R56 37 1 8R1 1 27R1

```

98R1 9Q98
-----6$$$ ARRAY IZMAT - MATERIAL NUMBER FOR EACH ZONE-(NZONES)---
6$$$
1 2 4 3 4 4 4 4 06 4 4 06 4 4 4 4 4 4 4 06 4 4 06 4 4 4 4 4 1 1 1
1 1 1 10 11 12 19R4 3 4
-----7$$$ ARRAY MATID - BU-LIBRARY XSEC SET ASSIGNMENTS-(NXTAPE)-
7$$$
-----8$$$ ARRAY REGION EDITS BY ZONE-(IEDIT X NZONES)-----
8$$$
-----EDIT #1-----
1 2 3 4 5 6 7 8 9 10 11 12 13 14 15 16 .7 18 19 20 21 22 23 24 25
26 27 28 29 30 31 32 33 34 35 36 37
38 39 40 41 42 43 44 45 46 47 48 49 50 51 52 53 54 55 56 57 58
-----EDIT 2 AVERAGE POWER IN EACH ELEMENT-----
1 2 3 4 5 6 7 8 9 10 11 12 13 14 15 16 17 18 19 20 21 22 23 24
25 26
27 28 29 29 29 30 31 32 33 34 35 26 27 28 18 19 21 22 24 25 10 13
14 15 16 17 5 6 7 8 57 58
-----EDIT 3 AVERAGE POWER ACROSS CORE -----
1 2 3 4 5 5 5 5 6 5 1 7 5 5 5 5 5 5 8 5 5 9 5 5 5 5 1 1 1
10 11 12 13 14 15 19R5 4 58
-----9** ARRAY FISSION SPECTRUM-(IGM)-----
9**
*FISSION SPECTRUM FROM ENDF/B IV GENERATED IN EPRI-CELL
* ENERGY BOUNDARIES - 10 MEV, 0.821 MEV, 5.53 EV, 0.625 EV, 0 EV
1.0 0.0
-----13** ARRAY CROSS SECTIONS FROM CARDS-(ITL X NGPS X NXCARD)-----
13**
* 2 GP REG NONLAT **** 93% HEU WATER REFLECTOR
0.0 4.58252E-04 0.0 2.65154E-01 2.15893E-01 0.0
0.0 1.87576E-02 0.0 2.09724E+00 2.07848E+00 4.88029E-02
* 2 GP REG NONLAT **** 93% HEU STANDARD ELEMENT SIDEPLATE
0.0 3.86035E-04 0.0 1.80141E-01 1.67355E-01 0.0
0.0 1.28098E-02 0.0 5.97867E-01 5.85057E-01 1.23995E-02
* 2 GP REG NONLAT **** 93% HEU DUMMY ELEMENT NON-FUELED
0.0 4.22391E-04 0.0 2.60253E-01 2.21962E-01 0.0
0.0 1.69640E-02 0.0 1.65508E+00 1.63811E+00 3.78687E-02
* 2 GP REG TOTAL **** 93% HEU STANDARD FUEL, CLAD, MODERATOR REGION
1.2[A88E-03 2.42961E-03 3.14696E-03 2.68234E-01 0.00000E-01 0.00000E+00
5.60711E-02 8.19225E-02 1.35636E-01 1.63013E+00 0.00000E+00 3.50072E-02
* 2 GP REG TOTAL **** 93% HEU CONTROL FUEL, CLAD, MODERATOR REGION
1.34364E-03 2.52650E-03 3.27171E-03 2.64068E-01 2.24750E-01 0.0
5.82553E-02 8.50610E-02 1.40920E-01 1.71259E+00 1.62753E+00 3.67917E-02
* 2 GP REG NONLAT **** 93% HEU GUIDE TUBE REGION
0.0 4.12352E-04 0.0 2.56560E-01 2.20295E-01 0.0
0.0 1.64707E-02 0.0 1.57236E+00 1.55589E+00 3.58520E-02
* 2 GP REG NONLAT **** 93% HEU GRAPHITE REFLECTOR
0.0 3.31330E-05 0.0 2.32656E-01 2.30476E-01 0.0
0.0 2.16348E-04 0.0 3.58813E-01 3.58596E-01 2.14693E-03
* 2 GP REG NONLAT **** 93% HEU ALUMINUM 6061
0.0 3.92668E-04 0.0 1.09891E-01 1.09382E-01 0.0
0.0 1.25551E-02 0.0 9.06178E-02 7.80627E-02 1.16865E-04
* 2 GP REG NONLAT **** 93% HEU LEAD FROM EPRI-CELL
0.0 1.49720E-04 0.0 3.07090E-01 0.33645 0.0

```

```

0.0      1.95330E-03 0.0      3.70060E-01 0.36936      1.81970E-04
' 2 GP REG NONLAT **** 93% HEU BARE RABBIT TUBE REGION
8.39352E-09 5.01512E-04 8.39352E-09 2.47598E-01 2.10037E-01 0.0
0.0      2.03414E-02 0.0      1.62419E+00 1.60385E+00 3.70592E-02
' 2 GRP CADMIUM RABBIT TUBE CROSS SECTION FROM EPRI-CELL
8.39352E-09 5.07182E-04 8.39352E-09 2.47598E-01 2.10037E-01 0.0
0.0      2.87380E-02 0.0      1.62419E+00 1.60385E+00 3.70592E-02
' 2 GP REG NONLAT **** 93% HEU CONTROL ELEMENT SIDE PLATE
0.0      3.78051E-04 0.0      1.63955E-01 1.54716E-01 0.0
0.0      1.21723E-02 0.0      4.45142E-01 4.32969E-01 8.86137E-03
' 2 GP REG NONLAT **** 93% HEU REGULATING ROD
1.34674E-07 2.09360E-03 1.34674E-07 2.80300E-01 2.60343E-01 0.0
0.0      7.85950E-02 0.0      1.15060E+00 1.07185E+00 1.78559E-02
' 2 GP REG NONLAT **** 93% HEU SHIM ROD WITH BORON
1.87221E-08 1.73950E-02 1.87221E-08 3.59780E-01 3.1760E-01 0.0
0.0      0.31346E+00 0.0      0.95059E+00 6.37223E-01 1.06183E-02
' 00% VOIDED WATER CROSS SECTIONS FOR THE PERIPHERY OF THE CORE
0.0      4.58252E-04 0.0      2.65154E-01 2.11893E-01 0.0
0.0      1.87576E-02 0.0      2.09724E+00 2.07848E+00 4.88029E-02
' 95% VOIDED WATER CROSS SECTIONS FOR THE PERIPHERY OF THE CORE
0.0      2.29110E-03 0.0      1.32577E-02 1.0947E-02 0.0
0.0      9.37880E-04 0.0      1.04862E-01 1.03924E-01 2.44015E-03
' 2 GP          93% HEU AL TO APPROXIMATE AIR X-SECS X 10-3
0.0      3.92668E-07 0.0      1.09491E-01 1.09382E-01 0.0
0.0      1.25551E-05 0.0      7.80630E-02 7.80627E-02 1.16865E-04
-----15** ARRAY BUCKLING MODIFIERS=(NZONES OR NZONES X NGRS)-----
15**
      F      1.0
-----17** ARRAY BURNUP IN % OF FISSILE=(NXTAPE)-----T!-----
17**
      BURNUP IN % OF FISSILE EDIT PROVIDED IN LEOPARD
      T
-----91$$ AND 92** ARRAYS TIME STEP CONTROL-----
      IBUCON  NPRT  NTUSD  IXSTR  IDUP17  IREGAD  E  T
91$$      0      1      0      00      0      0  E  T
92**  1.0E-10      1.0
/*
//

```

APPENDIX B

CROSS SECTION GENERATION AND CELL DISCRETIZATION

The two main inputs to LEOPARD are lattice geometry and material compositions. There are three regions that describe the LEOPARD lattice: a fuel region, clad and void region and moderator channel region. For slab geometry, lattice spacing is measured from the center of the fuel plate to the outside edge of the region. Information for U_3Si_2 was obtained from references 9 and 1. The B-1 shows the lattice descriptions for the HEU and LEU cores. The B-1 shows the number density or volume fraction for the different homogenized zones of the HEU and LEU cores. A trace amount of boron-10 is added to all regions containing aluminum for the LEU core to account for the impurities in AL 6061. Volume fractions for graphite and water reflectors, aluminum and lead in the thermal column were all 1.000. The cladding on the present HEU fuel plate is 20 mils (0.0508 cm) thick, and the cladding on the proposed LEU fuel plate will be only 15 mils (0.0381 cm) thick.

TABLE B-1

Lattice spacing for the HEU and proposed LEU cores (cm).

region	HEU	LEU
fuel material	0.0254	0.0254
clad	0.0762	0.0635
moderator	0.8103	0.4426

TABLE B-11

Number densities and volume fractions for the homogenized zones of the HEU and LEU cores.

Zone description	Isotope or material	Number density [#/barn/cm]	Volume fraction [.]
HEU fuel material	^{235}U	2.254E-3	
	^{238}U	2.472E-4	
	^{16}O	6.668E-3	
	Al		0.9037
HEU clad	Al		1.0077
HEU moderator	H_2O		1.0000
HEU standard element side plate	Al		0.7262
	H_2O		0.2738
HEU control element side plate	Al		0.7561
	H_2O		0.2439
HEU control guide tube	Al		0.1589
	H_2O		0.8411
HEU standard and control element end plate	^{235}U	1.829E-4	
	^{238}U	2.006E-5	
	^{16}O	5.411E-4	
	Al		0.2200
	H_2O		0.7566
LEU fuel material	^{235}U	1.761E-3	
	^{238}U	7.064E-3	
	^{10}B	2.539E-7	
	Al		0.8504
LEU clad	^{10}B	2.986E-7	
	Al		1.0077
LEU moderator	H_2O		1.0000
LEU standard element side plate	^{10}B	1.987E-7	
	Al		0.6654
	H_2O		0.3346
LEU control element side plate	^{10}B	2.414E-7	
	Al		0.8084
	H_2O		0.1916

TABLE B-II cont.

Zone description	Isotope or material	Number density [$\#/\text{barn}/\text{cm}$]	Volume fraction [-]
LEU control element guide tube	^{10}B	6.262E-8	
	Al		0.2097
	H_2O		0.7804
LEU standard and control element end plate	^{235}U	1.757E-4	
	^{238}U	7.048E-5	
	^{10}B	6.687E-8	
	Al		0.3088
	H_2O		0.6763

The computational model, in the Y-direction, for the thermal column consists of 1 inch of aluminum, 4 inches of lead, and 17 inches of graphite. The Y-mesh was 2 mesh lines (1.27 cm) in the aluminum, 4 mesh lines in the lead (2.54 cm), and 11 mesh lines in the graphite (some 2.54 and some 4.05 cm).

Figures B1 and B2 show the HEU standard and control elements, respectively, (reproduced from the UMRR blueprints). Figures B3 through B5 show the computational models of various elements used in this study.

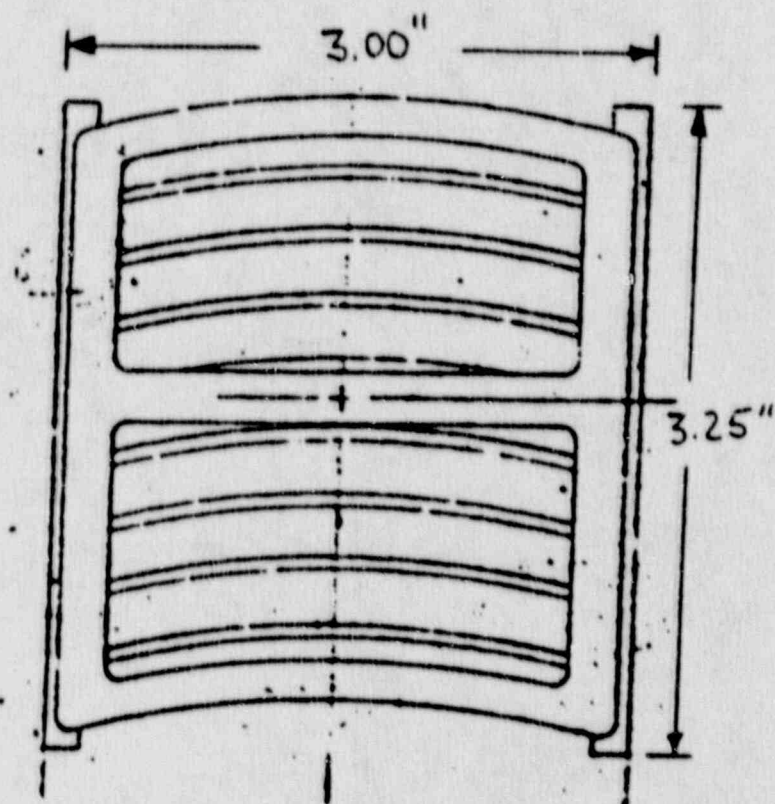


Fig. B1. The HEU standard element from UMRR blueprints (shown with top handle).

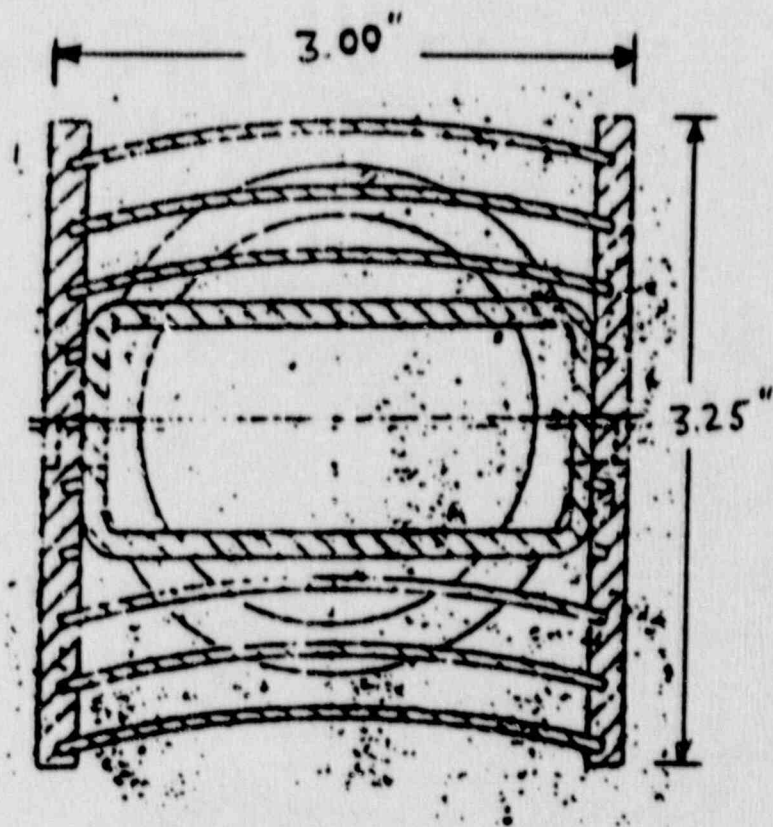


Fig. B2. The HEU control element from UMRR blueprints.

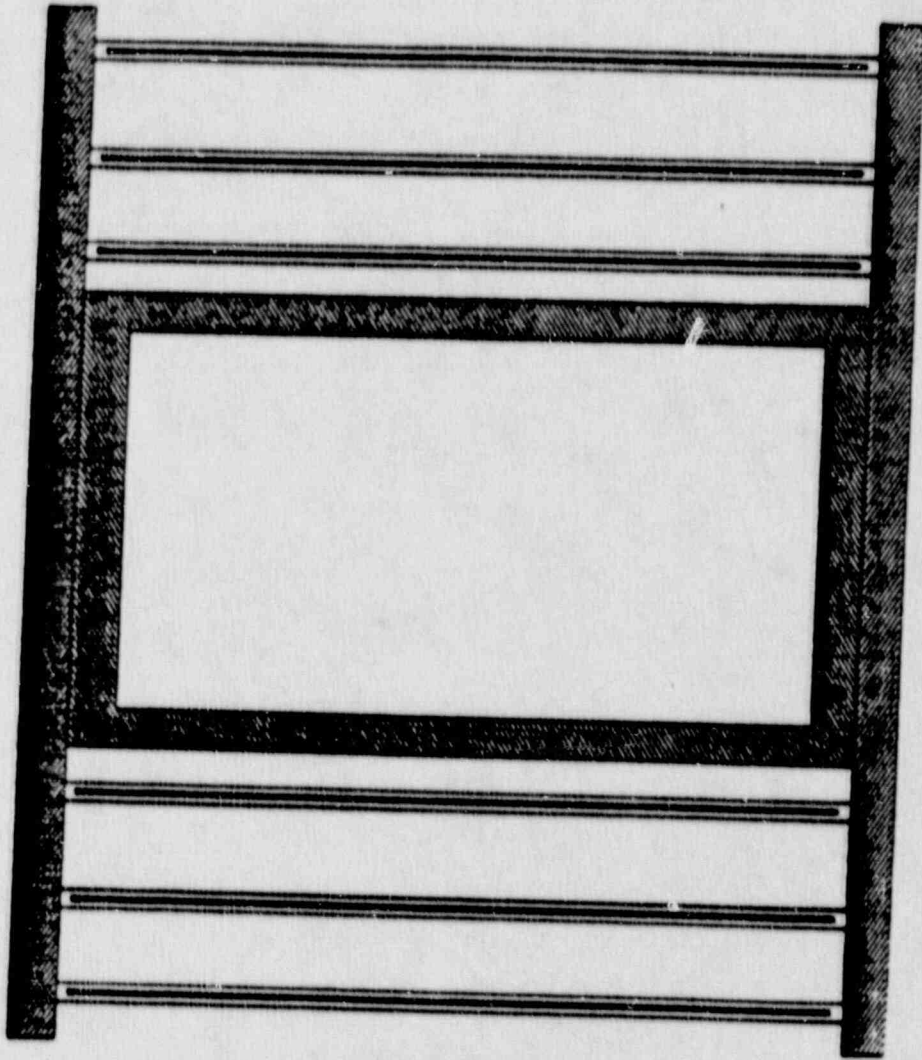


Fig. B3. The computational model for the HEU control element (not to scale).

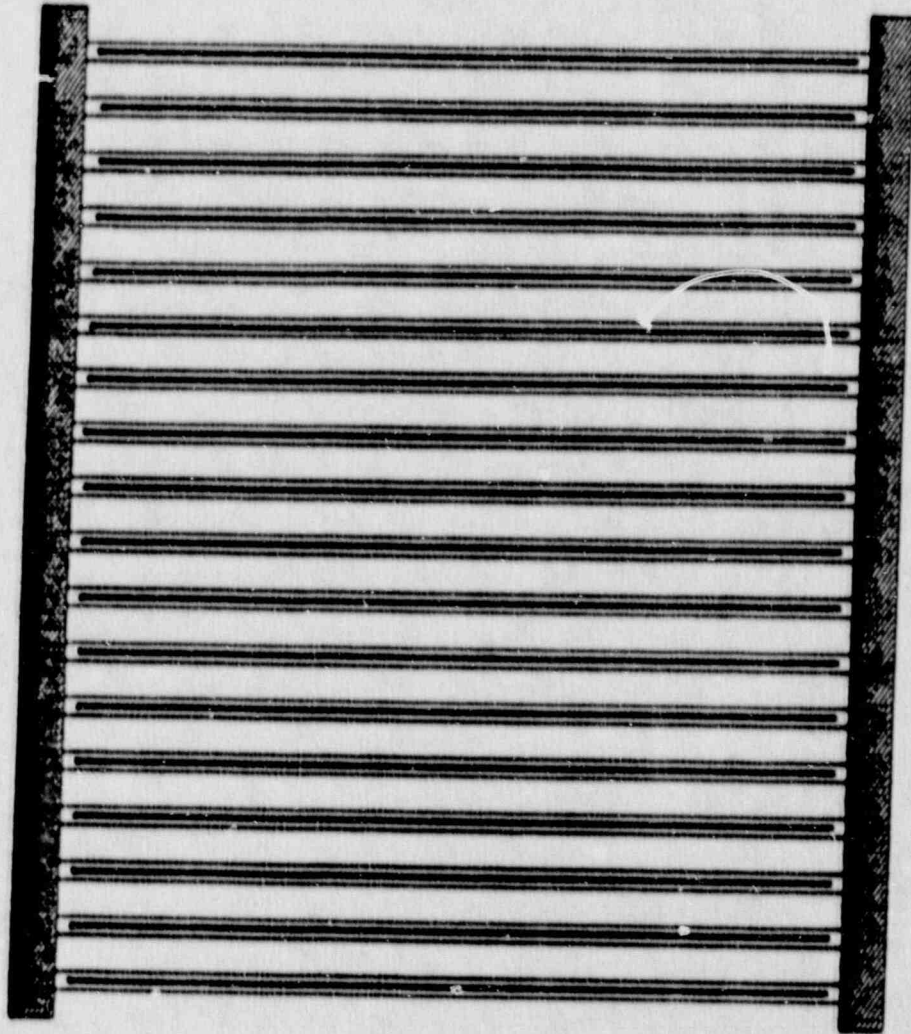


Fig. B4. The computational model for the LEU standard element (not to scale).

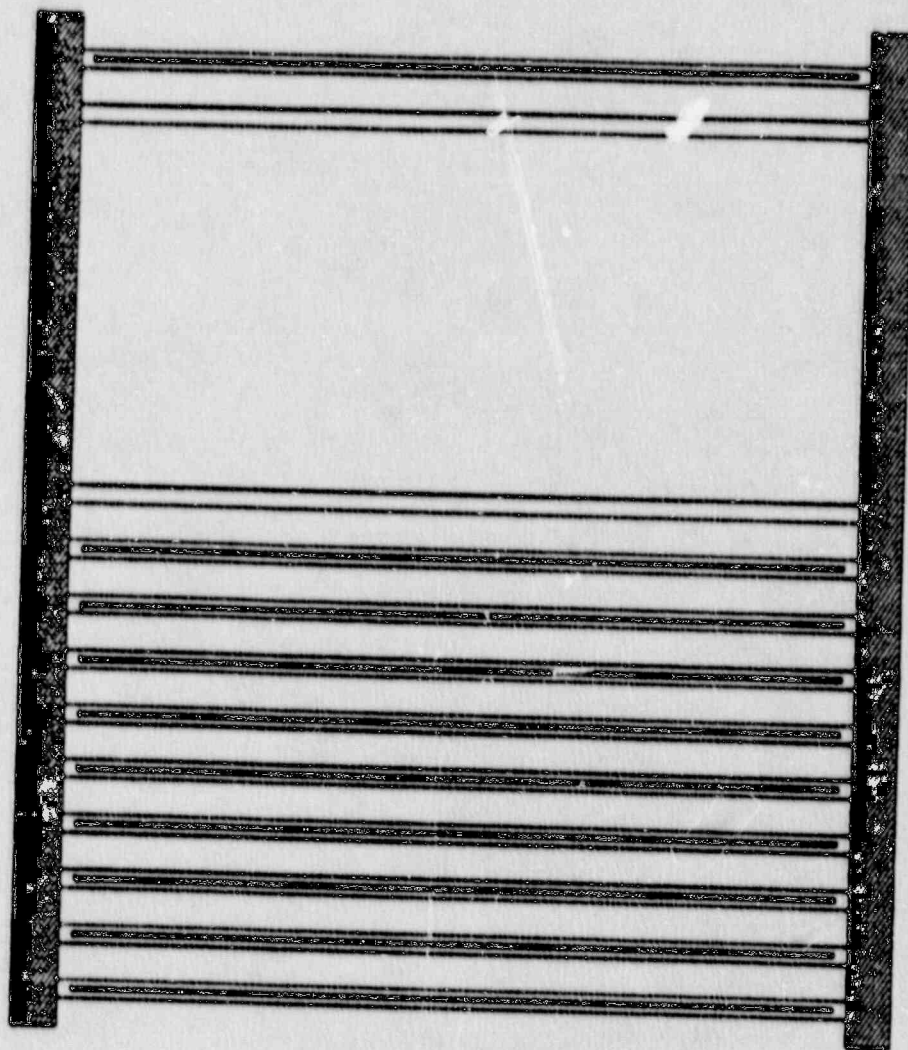


Fig. B5. The computational model for the LEU irradiation fuel element (not to scale).

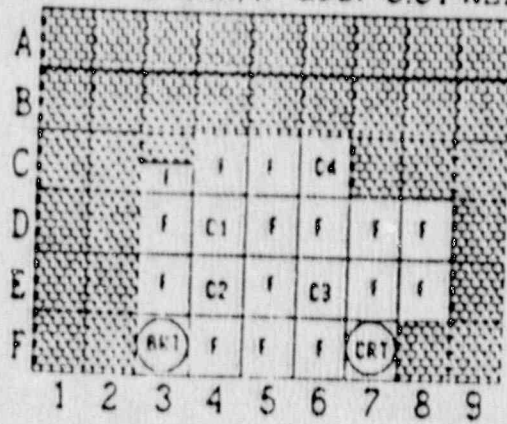
APPENDIX C

SELECTION OF A LEU CORE CONFIGURATION

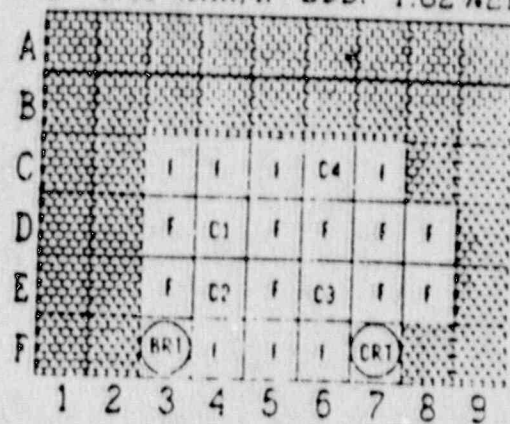
When the investigation to determine a new LEU element and LEU core began, the only constraint was that the element must be of the same outer dimensions as an HEU element so that it would fit into the grid plate. Two different elements were investigated: an element with 16 fuel plates and 2 outer aluminum plates, and an element with 18 fueled plates. The aluminum plates on the 16 plate element were added to better protect the thinly clad fuel plates of the element during handling. The 16 fuel plate element cores were typically determined to be 3 elements larger than cores constructed with the 18 fuel plate element. The different core configurations investigated are shown in Figures C1 and C2 for the 16 fuel plate element and the 18 fuel plate element, respectively.

It was decided by the reactor staff that the 18 fuel plate element would be the most suitable element and that core configuration (e) of Figure C2 would represent the proposed LEU core.

ANL: $-3.75\% \Delta k/k$ 2DB: $-3.51\% \Delta k/k$ ANL: $-1.45\% \Delta k/k$ 2DB: $-1.82\% \Delta k/k$

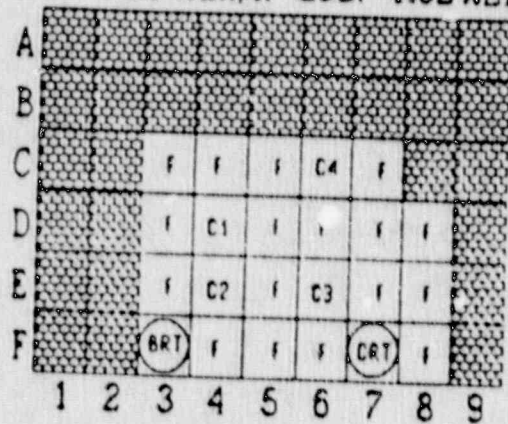


(a)

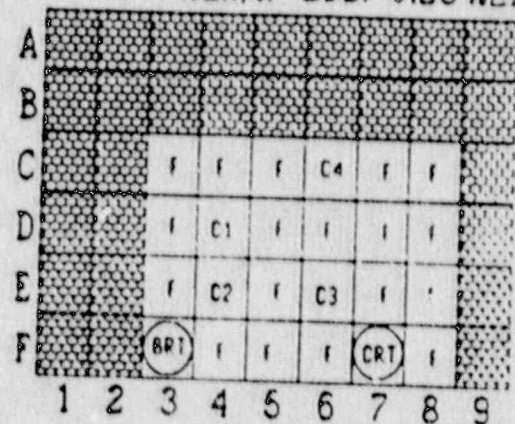


(b)

ANL: $-0.83\% \Delta k/k$ 2DB: $-1.52\% \Delta k/k$ ANL: $0.10\% \Delta k/k$ 2DB: $-0.28\% \Delta k/k$

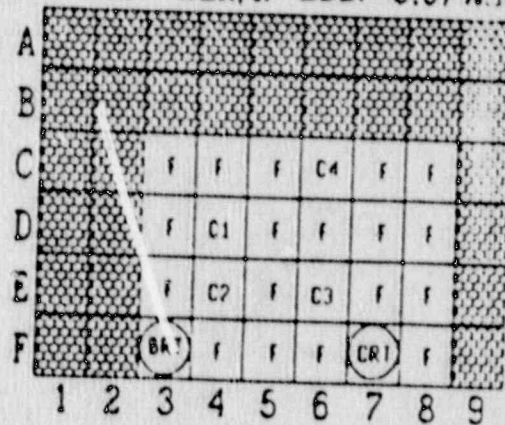


(c)



(d)

ANL: $0.37\% \Delta k/k$ 2DB: $-0.07\% \Delta k/k$

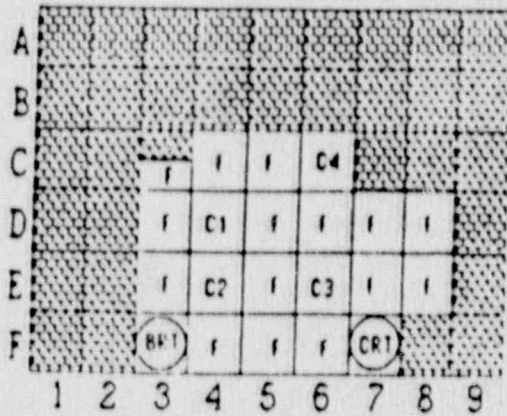


(e)

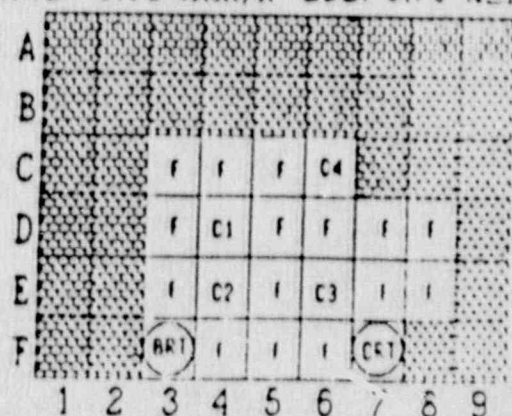
* T-MODE
CALCULATION

Fig. C1. The LEU cores investigated using the 16 fuel plate element

ANL: $-0.37\% \Delta k/k$ 2DB: $0.30\% \Delta k/k$ ANL: $-0.03\% \Delta k/k$ 2DB: $0.70\% \Delta k/k$

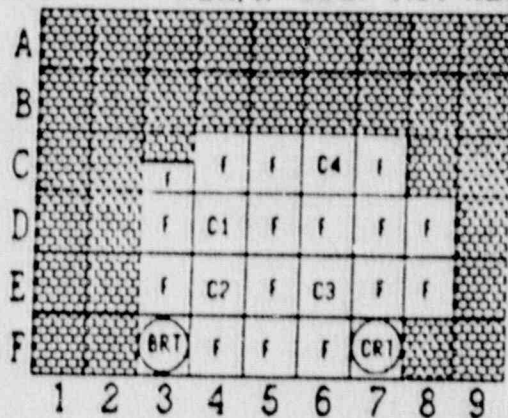


(a)

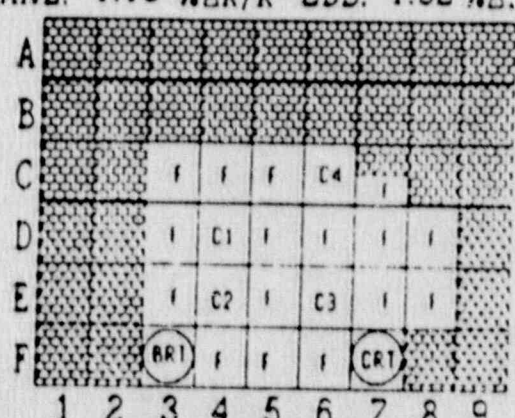


(b)

ANL: $1.40\% \Delta k/k$ 2DB: $1.91\% \Delta k/k$ ANL: $1.15\% \Delta k/k$ 2DB: $1.62\% \Delta k/k$

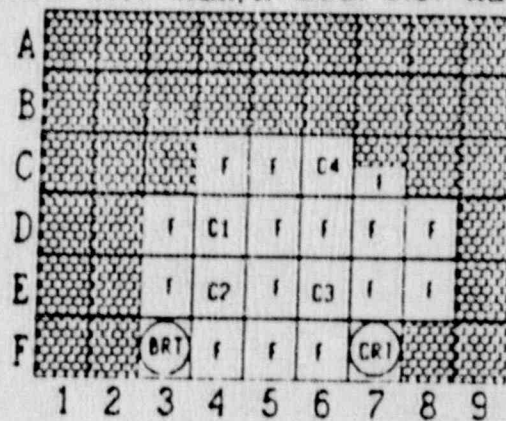


(c)



(d)

ANL: $0.17\% \Delta k/k$ 2DB: $0.87\% \Delta k/k$



(e)

Fig. C2. The LEU cores investigated using the 18 fuel plate element

APPENDIX D

CALCULATION OF POWER PEAKING FACTORS AND POWER DISTRIBUTIONS

The power peaking factor was calculated by dividing it into its radial, elemental, and axial components. The definitions of these components are given in Table D-I.

TABLE D-I

Power peaking factor definitions.

P.P. radial	-	$\frac{\text{Power generated in element}}{\text{Average power per element in the core}}$
P.P. axial	-	$\frac{\text{Maximum power generated in the axial direction}}{\text{Average power generated in axial direction}}$
P.P. element	-	$\frac{\text{Local maximum power generated at } z}{\text{Average power generated at } z}$
P.P. total	-	$\frac{\text{Peak power in element}}{\text{Average power in the core}}$
$\text{P.P. total} = \text{P.P. radial} * \text{P.P. element} * \text{P.P. axial}$		

The radial power peaking factor was determined by selecting edits in 2DB-UM that perform the averaging of the power in individual elements and in the entire core. The elemental power peaking factor calculation required scanning each mesh interval in the element for the maximum value for the thermal flux. The area of this mesh interval was calculated and the peak power density determined by summing the product of the flux and fission cross section for each energy group and dividing by the area. The average

power density was determined by 2DB-UM edits described above for the radial power peaking factor. The axial power peaking factor was determined by using a chopped cosine representation of the power distribution. It was assumed the same for all elements in the core. Power distributions were determined by selecting a different set of edits for 2DB-UM.

On the following pages, Figures B1 through B4 show the power peaking factors and power distributions for the HEU and proposed LEU cores. Figure B5 shows the measured relative thermal flux for the current HEU core. The values for the thermal flux were normalized to 1.0×10^{12} n/cm²/s. It was from comparison of this figure to the calculated HEU power distribution that led to the investigation of the flattening of the thermal flux (thermal flux is directly proportional to power).

	1	2	3	4	5	6	7	8	9
A									
B									
C			0.85 1.17 1.33	0.95 1.20 1.52	0.99 1.13 1.49	Reg.			
D			0.92 1.25 1.53	C1	1.15 1.13 1.73	1.11 1.12 1.65	1.03 1.20 1.65	0.84 1.34 1.50	
E			0.90 1.25 1.49	C2	1.15 1.13 1.73	C3	1.01 1.28 1.72	0.83 1.25 1.38	
F			BRT	0.91 1.33 1.61	0.99 1.28 1.68	0.93 1.33 1.65	CRT		

Axial=1.33

Radial	1.18	1.18	1.21	1.02
Element	1.22	1.23	1.24	1.30
Total	1.91	1.94	2.00	1.76
	C1	C2	C3	REG.

Fig. D1. HEU core power peaking factors.

	1	2	3	4	5	6	7	8	9
A									
B									
C				0.89 1.38 1.63	0.95 1.39 1.76	Reg.	0.96 1.46 1.86		
D			0.87 1.30 1.51	C1	1.07 1.30 1.84	1.05 1.23 1.72	0.96 1.27 1.62	0.85 1.45 1.64	
E			0.86 1.41 1.61	C2	1.09 1.32 1.91	C3	0.99 1.37 1.80	0.83 1.47 1.62	
F			BRT	0.89 1.40 1.66	0.94 1.38 1.72	0.92 1.36 1.67	CRT		

Axial=1.33

Radial	1.17
Element	1.32
Total	2.06

C1

Radial	1.16
Element	1.33
Total	2.06

C2

Radial	1.24
Element	1.35
Total	2.22

C3

Radial	1.11
Element	1.26
Total	1.86

REG.

Fig. D2. Proposed LEU core power peaking factors.

	1	2	3	4	5	6	7	8	9
A									
B									
C			5.01 2.51	11.20 5.60	11.70 5.85	Reg.			
D			10.90 5.45	C1 13.66 6.83	13.10 6.55	12.17 6.09	3.89 4.94		
E			10.65 5.32	C2 13.78 6.89	C3 11.98 5.99	9.86 4.93			
F			BRT 5.39	10.79 5.86	11.17 5.51	11.03 5.51	CRT		

Kilowatts	8.41	8.27	8.61	7.27
% Power	4.21	4.13	4.31	3.64
	C1	C2	C3	REG.

Fig. D3. HEU core power distribution.

	1	2	3	4	5	6	7	8	9
A									
B									
C				10.98 5.49	11.68 5.84	Reg.	5.88 2.94		
D			10.74 5.37	C1	13.18 6.59	12.94 6.47	11.80 5.90	10.54 5.27	
E			10.64 5.32	C2	13.44 6.72	C3	12.18 6.09	10.24 5.12	
F			BRT	10.94 5.47	11.58 5.79	11.26 5.63	CRT		

Kilowatts	7.96	7.94	8.46	7.58
% Power	3.98	3.97	4.23	3.79
	C1	C2	C3	REG.

Fig. D4. Proposed LEU core power distribution.

	1	2	3	4	5	6	7	8	9
A									
B				0.55	S	0.55			
C		0.35	0.67	1.80	3.10	Reg.	0.82	0.19	
D		0.53	1.70	C1	3.30	2.80	2.00	1.30	0.36
E			2.20	C2	5.00	C3	3.30	2.00	
F			2.40	1.40	3.00	0.63	0.10		

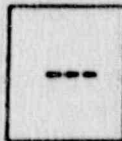
			
C1	C2	C3	REG.

Fig. D5. Measured relative thermal flux of the HEU UMRR.

APPENDIX E

CALCULATIONS OF REACTIVITY COEFFICIENTS

The temperature coefficient of the moderator is the sum of two component coefficients, the moderator density coefficient and moderator temperature coefficient. The moderator density coefficient is due to changing only the density of the moderator. The moderator density coefficient is shown in Figure E1 for the HEU and LEU cores. The moderator temperature coefficient is due to changing only the temperature of the moderator. The moderator temperature coefficient is shown in Figure E2 for the HEU and LEU cores. The summing of the individual coefficients to get the total moderator are shown in Figures E3 and E4 for the HEU and LEU cores, respectively.

The Doppler coefficient is due to the resonance absorption in ^{238}U . Increased fuel temperature causes a broadening of the resonance peaks and hence increased absorption during the slowing down of the neutron. There is no measurable or calculable Doppler coefficient for the HEU core because of the relatively small amount of ^{238}U . Figure E5 shows the calculated Doppler coefficient for the proposed LEU core.

The reactivity worth of a 2.31 cm^2 void at the midcore position E-5 for the HEU is shown in Figure E6. This figure shows the two methods used in modeling a void: the slow reduction in the number density in water and the use of adjusted aluminum cross sections. Both methods appear to show a positive reactivity for the void. Since the void coefficient has never been measured for an interior core position, no comparison could be made to measured data.

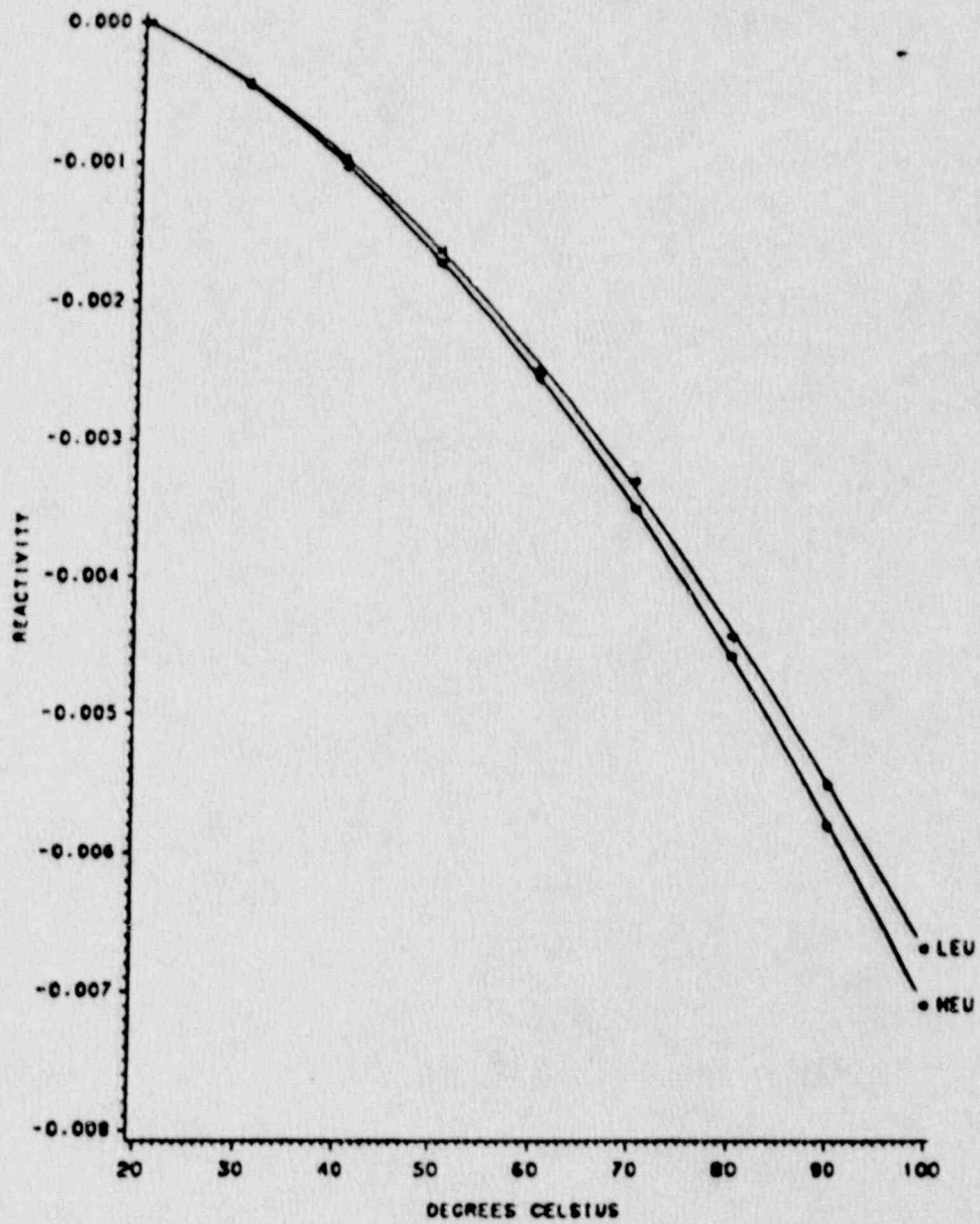


Fig. E1. Moderator density coefficient versus temperature for HEU and proposed LEU cores.

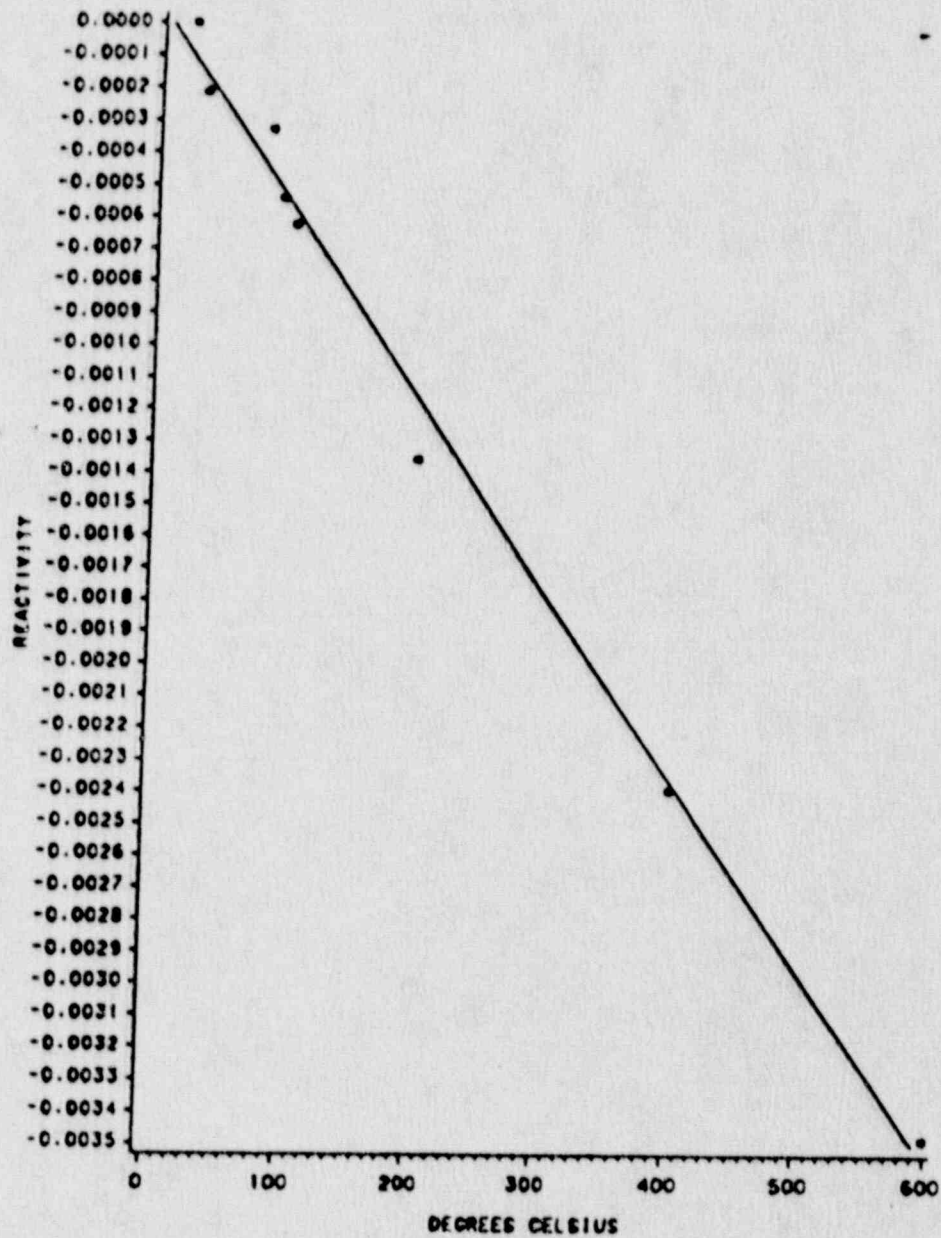


Fig. E5. Doppler coefficient versus temperature for proposed LEU core.

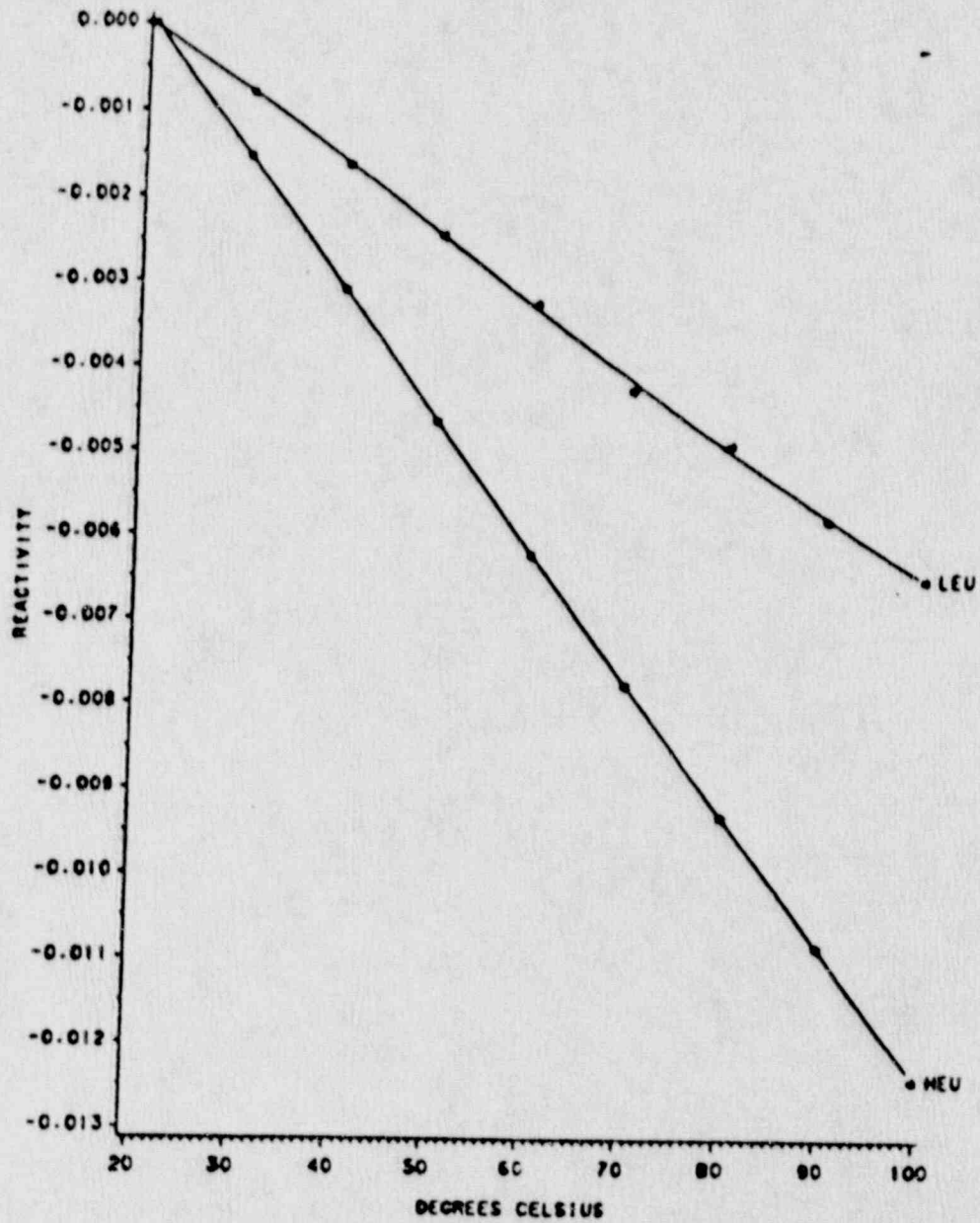


Fig. E2. Moderator temperature coefficient versus temperature for HEU and proposed LEU cores.

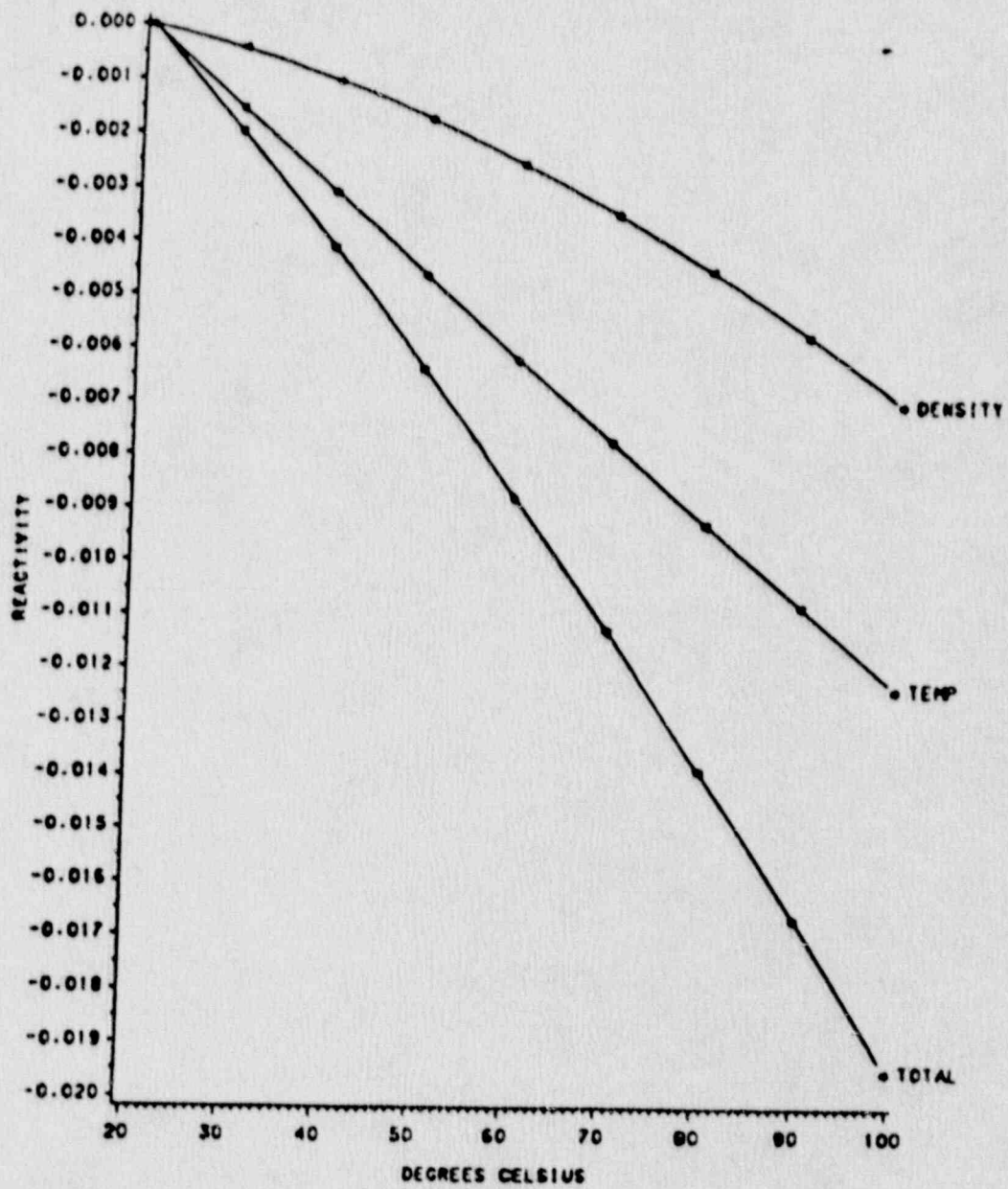


Fig. E3. Moderator coefficients versus temperature for HEU Core.

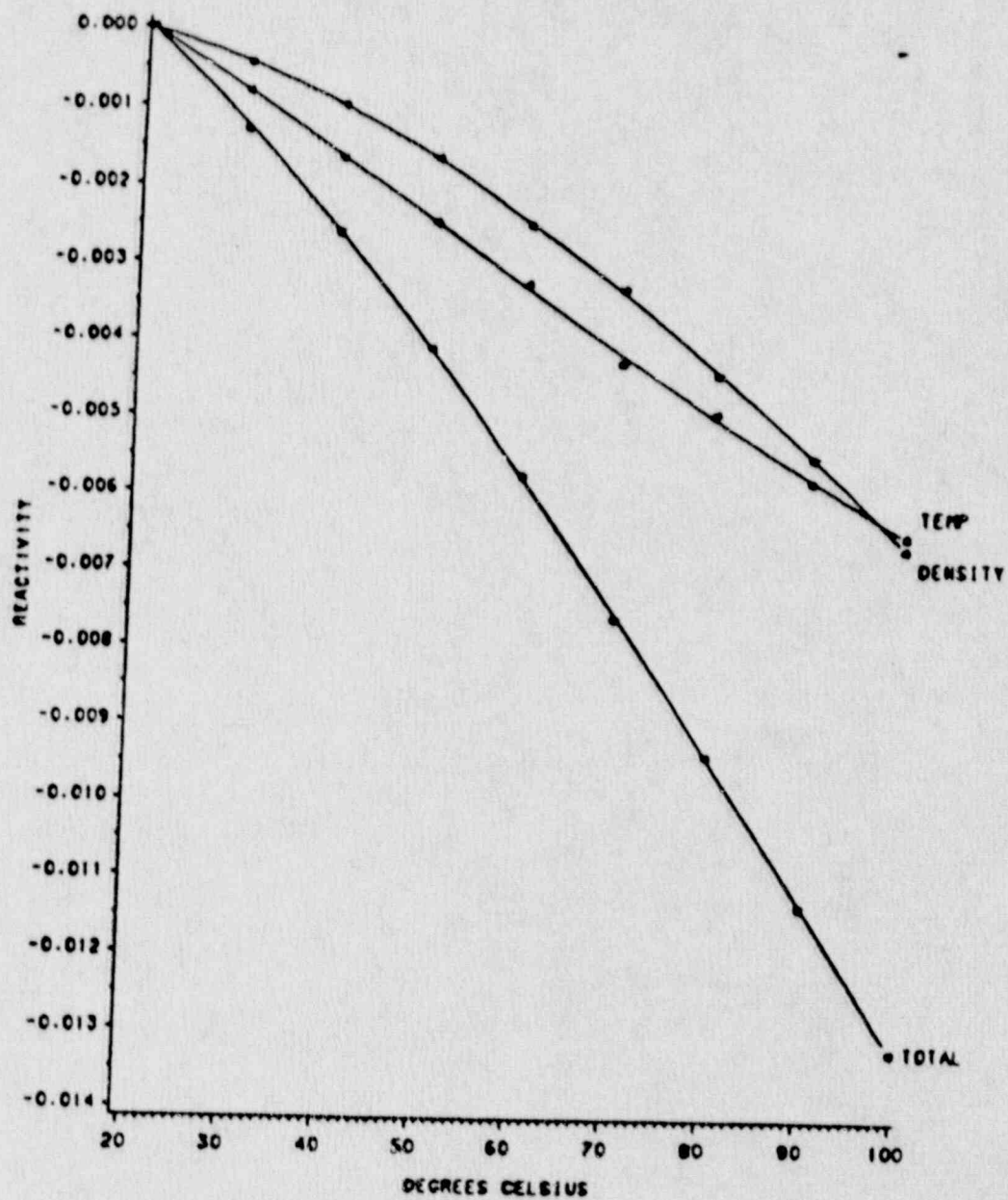


Fig. E4. Moderator coefficients versus temperature for LEU Core.

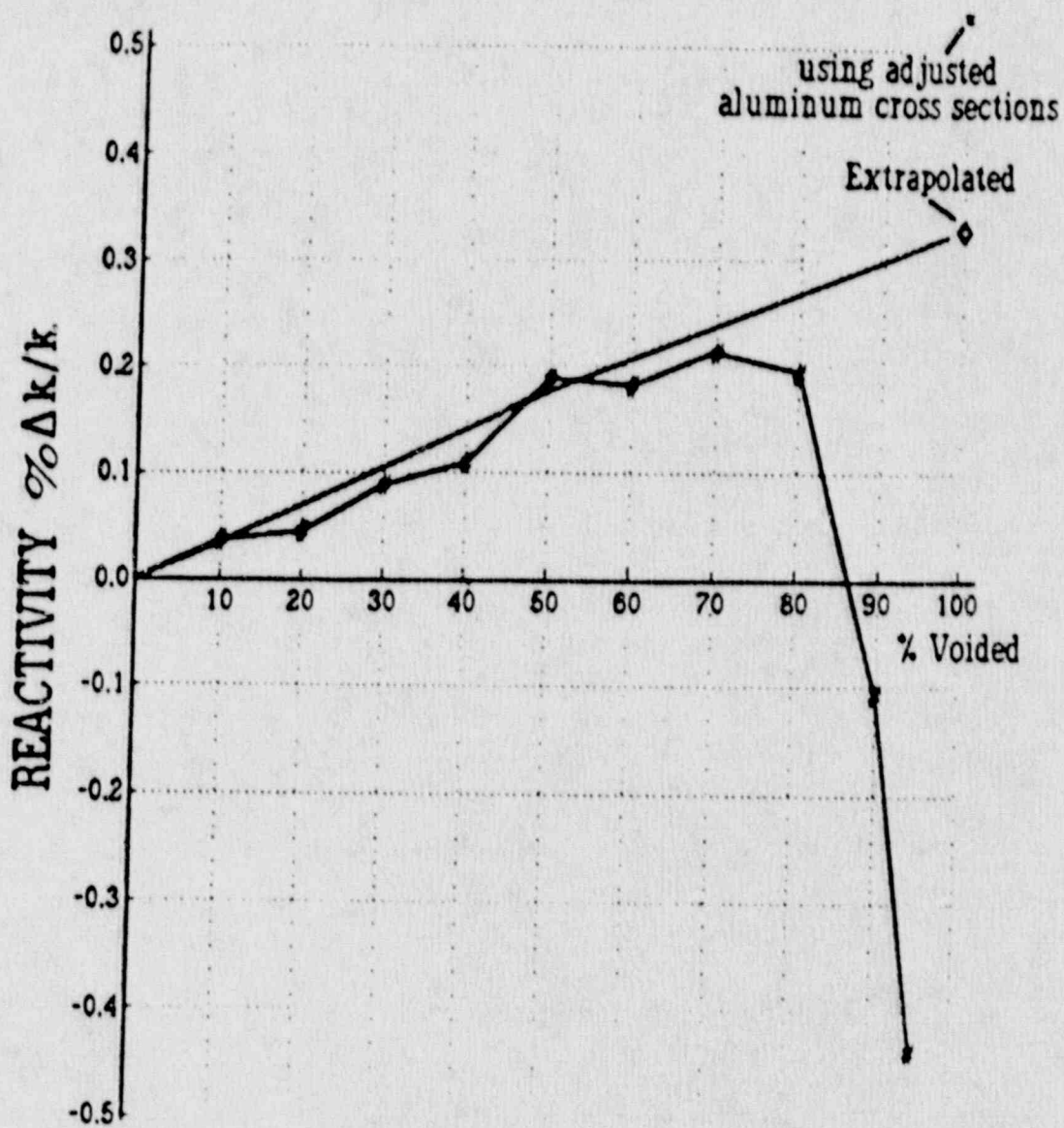


Fig. E6. Reactivity worth of a mid-core void versus percent voiding of water for the HEU core.

APPENDIX F

METHODS TO CALCULATE REACTIVITY WORTHS OF CONTROL RODS

Direct reactivity calculations of highly absorbing control rods are impossible for neutron diffusion codes. An approximation for control rod behavior can be made by performing a reaction rate matching between a Monte Carlo code calculation and a diffusion code as described in reference (11).

The first step is to create a unit cell consisting of a control rod element surrounded by 8 standard fuel elements using reflective boundary conditions on the four sides. This unit cell is the geometry used in both codes. The Monte Carlo code is run once and the ratio of the absorption rate in the control rod (control rod + water in guide tube + guide tube) and the fission rate in the rest of the unit cell (fuel + moderator + clad + sideplates) is then determined for each energy group that will be used in the diffusion code.

$$\frac{R_a |_{\text{rod}}}{R_f |_{\text{cell}}} = \frac{\Sigma_a * \phi * V |_{\text{rod}}}{\Sigma_f * \phi * V |_{\text{cell}}} \quad (\text{F-1})$$

These reaction rates as determined by the Monte Carlo code are the base rates that will be matched by the diffusion code.

Initial diffusion cross sections are generated by a cross section collapse code (LEOPARD) for all regions in the unit cell including the homogenized control rod - guide tube region. The diffusion code is then run with these initial cross sections and the reaction rate ratios are calculated in each energy group. The

following is the stepwise method used to match all group reaction rate ratios:

1. Run diffusion code and determine reaction rate ratios for each energy group.
2. Start with the highest energy group and proceed down through each energy group.
3. Calculate the new Σ_a and Σ_{tr} for the control rod region for the current energy group as follows;

$$\Sigma_a |_{new} = \frac{R_a}{R_f \text{ MC}} * \frac{R_f |_{cell}}{\phi * V |_{rod}} \quad \text{2DB-UM} \quad (\text{F-2})$$

$$\Delta\Sigma_a = \Sigma_a |_{new} - \Sigma_a |_{old} \quad (\text{F-3})$$

$$\Sigma_{tr} |_{new} = \Sigma_{tr} |_{old} + \Delta\Sigma_a \quad (\text{F-4})$$

4. Rerun the diffusion code replacing the old absorption and transport cross sections with the new values.
5. Repeat steps 3 and 4 until the reaction rate ratios for the current energy group match for both the diffusion and Monte Carlo codes. Then proceed to the next lower energy group and repeat steps 3 and 4. Repeat process for all energy groups.
6. The process of sweeping down through the energy groups has the effect of slightly changing the reaction rates in all the other energy groups. Because the reaction rates in the higher energy groups have changed steps 2 through 5 must be repeated until there is convergence of ratios in all energy groups.

Results of the reaction rate matching method calculations for the HEU core are shown in Table F-I.

TABLE F-1

Calculated and measured control rod worths
for the UMRR HEU core ($\% \Delta k/k$).

rod	calculated	measured
C-1	-2.799	-2.64
C-2	-2.712	-2.65
C-3	-2.859	-3.35
reg.	-0.744	-0.35

Rod worths for rods 1 and 2 compare favorably with measured data, while rod worths for rod 3 and the regulating rod are significantly different. The cause of this difference arises from the assumptions of using the unit cell geometry to calculate adjusted cross section as described in the previous section. The relatively small HEU core has a large spatial dependence of the flux and hence the reaction rates vary considerably locally. In the case of the shim rods only one unit cell calculation was performed and the same initially generated cross sections were used in all three shim rods, causing the calculated reactive worths of the rods to be similar. The large difference in the case of the regulating rod is because the geometry of the unit cell is much too different from the global calculation. In the unitcell, the regulating rod is surrounded by 8 standard fuel elements with reflective boundary conditions on all sides (no X-Y flux gradient). In the global calculation, the regulating rod is at the edge of the core and is surrounded by 4 standard fuel elements on one side and 4 water cells on the other side, a significant flux gradient is present in this geometry.

To eliminate the effects of geometry in the reaction rate matching method the complete global geometry must be used for both the Monte Carlo and diffusion codes. Changing to the global geometry

will significantly increase the time to determine the adjusted cross sections because of the increased computer time and the neutronic coupling of the control rods. This increased time is undesirable but seems the only way to achieve accurate results. -

Since the regulating rod is a stainless steel 304 tube filled with water and the SS 304 is homogenized across the entire rod region, the cross sections generated by the cross section collapse code (LEOPARD) should give adequate results. The unadjusted cross sections were used in a global calculation and the results are in good comparison with the known worth of the regulating rod. The results are in Table F-II.

TABLE F-II

Calculated and measured worth of the regulating rod in the HEU core ($\% \Delta k/k$).

rod	calculated	measured
reg.	-0.31	-0.35

APPENDIX G

ADDITIONAL REACTIVITY CALCULATIONS

The reactivity of a standard element on the periphery of the core was determined for both the HEU and LEU cores. The position of the element in the HEU core was C-7 and C-3 for the proposed LEU core. The reactivity worth for the HEU core was 1.48% and 0.95% for the LEU core.

Table G-I shows the various Irradiation Fuel (IF) element designs that were investigated along with the power peaking factor (P.P.) and thermal flux values. The IF was inserted in position E-5 of the grid plate

TABLE G-I

Various irradiation fuel element designs, power peaking factors and thermal fluxes in grid position E-5.

# of Fueled plates removed	# of Al plates added	width of trap (cm)	Total P.P. in IF	Total P.P. in E-6	Peak Thermal flux in IF	Average Thermal flux in IF	k_{eff}
2	0	1.202	2.02	2.17	2.20+12	2.07+12	1.0090
4	0	2.088	2.20	2.20	2.85+12	2.57+12	1.0082
4	2	1.202	2.12	2.18	2.65+12	2.61+12	1.0063
6	0	2.970	2.29	2.28	3.40+12	3.09+12	0.9994
6	2	2.088	2.26	2.25	3.20+12	3.04+12	0.9992
8	0	3.750	2.38	2.36	3.90+12	3.41+12	0.9923
8	2	2.970	2.31	2.31	3.70+12	3.36+12	0.9873
10	2	3.750	2.43	2.36	3.95+12	3.48+12	0.9845
all	---	---	----	2.71	5.20+12	3.71+12	0.9689
none	---	---	1.91	2.22	---	---	1.0124

An experiment was performed using the Core Access (CA) element. The experiment was split into two runs on two different days. The first was on 10/23/87 with the CA being filled with air, and the second run was on 11/4/87 with the water filled. For reasons of

comparison, measurements of the shim heights was performed in two different manners. The first was to set all shim rods to the same height. The second method was to set shim rods 1 and 3 to the same height and adjust shim rod 2 to achieve criticality. The results are in the following tables.

TABLE G-II

Raw data for CA experiment.

		Control Rod Heights (inches)			reg.	rho excess
		1	2	3		
<u>10/23/87</u>						
<u>inlet temp 68 F</u>						
No CA	1.)	21.12	21.12	21.12	24.0	0.405 %
	2.)	21.00	21.44	21.00	24.0	0.400 %
CA with air	1.)	20.12	20.12	20.12	24.0	0.670 %
	2.)	21.00	18.60	21.00	24.0	0.665 %
<u>11/4/87</u>						
<u>inlet temp 70 F</u>						
No CA	1.)	21.18	21.18	21.18	24.0	0.390 %
	2.)	21.00	21.63	21.00	24.0	0.385 %
CA with water	1.)	19.63	19.63	19.63	24.0	0.825 %
	2.)	21.00	17.55	21.00	24.0	0.800 %

TABLE G-III

Reactivity of Core Access element for normal (air-filled) and flooded conditions. Cases A and B are experimental data and 2DB-UM are from computer modeling ($\beta\Delta k/k$).

	CASE A	CASE B	2DB-UM
CA with air	0.265	0.265	0.421
CA with H2O	0.435	0.415	0.479